

# Stabilization of Nonlinear Systems with State-Dependent Representation: From Model-Based to Direct Data-Driven Control

Lidong Li, Rui Huang, and Lin Zhao

**Abstract**—This paper presents a novel framework for stabilizing nonlinear systems represented in state-dependent form. We first reformulate the nonlinear dynamics as a state-dependent parameter-varying model and synthesize a stabilizing controller offline via tractable linear matrix inequalities (LMIs). The resulting controller guarantees local exponential stability, maintains robustness against disturbances, and provides an estimate of the region of attraction under input saturation. We then extend the formulation to the direct data-driven setting, where a known library of basis functions represents the dynamics with unknown coefficients consistent with noisy experimental data. By leveraging Petersen’s lemma, we derive data-dependent LMIs that ensure stability and robustness for all systems compatible with the data. Numerical and physical experimental results validate that our approach achieves rigorous end-to-end guarantees on stability, robustness, and safety directly from finite data without explicit model identification.

**Index Terms**—nonlinear systems, state-dependent representation, data-driven control, region of attraction, robustness against disturbances, input saturation

## I. INTRODUCTION

The analysis and control of nonlinear systems are difficult, especially when the mathematical models describing the system dynamics are unavailable. In such cases, data-based control frameworks provide a way to reduce reliance on system models. One framework, known as indirect data-based control, first identifies the model from data and then applies model-based control. Another framework is direct data-driven control, which synthesizes controllers directly from data without explicitly identifying the system model. These approaches include adaptive control [1], virtual reference feedback tuning [2], iterative learning control [3], and reinforcement learning [4]. For a comprehensive overview, we refer interested readers to the survey articles [5]–[7]. Among direct data-driven approaches, those built on Willems *et al.*’s fundamental lemma (hereafter referred to as fundamental lemma) [8] have attracted growing interest and been extensively studied for linear time-invariant (LTI) systems [9]–[13]. These approaches can provide stability, robustness, optimality, safety, and many other desirable guarantees. However, extending linear results to nonlinear systems remains challenging, and theoretical guarantees may fail to generalize due to the intricacies of nonlinear dynamics.

### Review of Fundamental-Lemma-Based Methods

By utilizing the fundamental lemma, [9] represents LTI systems via their finite input-state data and solves data-dependent linear matrix inequalities (LMIs) to obtain a controller. It has

Lidong Li, Rui Huang, and Lin Zhao are with the Department of Electrical and Computer Engineering, National University of Singapore, Singapore 117583 (e-mail: {li.ld, ruihuang, elezhli}@nus.edu.sg).

also been extended to nonlinear systems by approximating the dynamics as a first-order linear term, while treating the remaining nonlinear part as process noise. The resulting controller guarantees local stability [9]. However, this approach requires restrictive assumptions on the remainder term, and does not provide an estimate of the region of attraction. The approaches in [14]–[17] addressed polynomial systems and developed globally asymptotically stabilizing controllers using sum-of-squares (SOS) programming; however, the SOS tool often suffers from scalability issues, high computational cost, and numerical sensitivity in practice. Other works addressing more general nonlinear systems typically employ various function approximations, such as polynomials [18]–[20], Gaussian processes [21], or kernel regression [22], [23]. These approximations are typically local [24], and the resulting controllers can be conservative due to approximation errors and data noise. The Koopman operator paradigm can provide a global linearization of the nonlinear system but rely critically on the choice of observable functions and the accuracy of finite-dimensional truncations [25], which may limit stability and robustness guarantees for strongly nonlinear or high-dimensional systems [26], [27]. Moreover, recent works also assume a library of known basis functions for unknown nonlinear vector fields to avoid analyzing approximation errors. It is employed in polynomial systems [17], data-driven feedback linearization [28]–[30], and nonlinearity cancellation via data [31]–[34]. The aforementioned methods construct data-driven controllers from a batch of data in an offline manner. In contrast, [35] introduces an online iterative control scheme, in which a state-dependent Riccati equation is solved through data-based LMIs at each control step. Yet, the feasibility of online LMIs is not guaranteed during runtime. This issue has been partially addressed in [36] in the case of noise-free data.

Despite extensive research over the years [13], [24], [32], direct data-driven nonlinear control remains an open problem. The key challenges include designing controllers with guaranteed stability from finite data samples and estimating the region of attraction through computationally tractable algorithms. Furthermore, data noise is inevitable and induces uncertainties in data-driven control. The control law should ensure robustness to such uncertainties. Other closed-loop properties from data, such as input-to-state stability [37, §7] [38] and region of attraction subject to input saturation [37, §8.2] [39], are important yet remain underexplored for nonlinear systems without model knowledge.

### Contributions

In this paper, we first propose a new model-based controller design method using the state-dependent representation of the nonlinear system. For this type of representation, model-based

method typically treats the nonlinear system as a linear system at each control step, and the controller is then obtained by solving state-dependent Riccati equation online [40]. However, a heuristic extension of this method to the data-driven case often suffers from recursive infeasibility, especially when the data is affected by noise. In contrast, our approach views this representation as a form of state-dependent parameter-varying model and incorporates robust control techniques to synthesize the controller offline. The resulting controller guarantees local stability, with an accompanying estimate of the region of attraction. The robustness of the closed-loop system against disturbances is rigorously analyzed. The region of attraction, taking into account input saturation, is also investigated.

We further extend the model-based method to direct data-driven controller design. We assume a library of known basis functions, and the state-dependent representation can be expressed as a linear combination of them, where the coefficients are unknown. Due to noise in the experimental data, there exists a set of coefficients consistent with the data. Since the true coefficients are unlikely to be distinguished, the controller should stabilize all systems in the data-consistent set. To this end, we make use of the Petersen's lemma [15] and directly synthesize the controller from data-dependent LMIs conveniently. The closed-loop properties, as discussed in the model-based case, can also be analyzed solely from data.

We summarize the main contributions as follows.

- Our controller is directly synthesized from noisy data. We not only ensure stability guarantees, but also provide data-driven analyses of robustness of the closed-loop system against disturbances and the estimate of the region of attraction under input saturation. Such analyses are rarely found in the literature on data-driven nonlinear system control.
- Our framework is applicable to more general nonlinear systems than feedback linearization and nonlinearity cancellation methods, which is demonstrated via numerical examples.
- Compared to solving the state-dependent Riccati equation online, our framework designs the controller offline, thereby avoiding the issue of recursive infeasibility that may arise during online operation.

### Outline

Section II presents the model-based controller design. Specifically, Section II-A introduces relevant preliminaries. Model-based stabilizing controller and the accompanying estimate of region of attraction is presented in Section II-B. Section II-C analyzes the robustness of the closed-loop system against disturbances. Section II-D designs the controller for systems with input saturation. Section III adapts the model-based controller design to the direct data-driven framework. Specifically, Section III-A includes relevant preliminaries. Data-driven stabilizing controller and the associated estimate of region of attraction is presented in Section III-B. Section III-C analyzes the robustness of the closed-loop system from data. Section III-D considers the system subject to input saturation. The estimate of region of attraction is revisited and discussed in Section III-E. To highlight our contributions, we conduct a thorough comparison with existing methods

in Section IV, covering both literature review and numerical evaluation. Finally, our method is validated by a physical experiment in Section V. All experimental codes, data and demonstrations are available at [41].

### Notation and Definition

Denote the set of real numbers as  $\mathbb{R}$ , and the set of natural numbers as  $\mathbb{N}$ . The identity matrix of size  $n$  and the zero matrix of size  $m \times n$  are denoted by  $I_n$  and  $0_{m \times n}$ : the indices are dropped when no confusion arises. Let  $(v_1, \dots, v_n)$  denote the stacked vector  $[v_1^\top \dots v_n^\top]^\top$ . For a symmetric matrix  $M$ ,  $\lambda_{\max}(M)$  and  $\lambda_{\min}(M)$  denote the largest and smallest eigenvalue of  $M$ . The 2-norm of a vector  $v$  is  $\|v\|$ , and the induced 2-norm of a matrix  $M$  is  $\|M\|$ . For matrices  $M$ ,  $N$  and  $O$  of compatible dimensions, we abbreviate  $MNO(MN)^\top$  to  $MN \cdot O[*]^\top$  or  $(MN)^\top OMN$  to  $[*]^\top O \cdot MN$ , where the dot clarifies unambiguously that  $MN$  are the terms to be transposed. For a symmetric matrix  $\begin{bmatrix} M & N \\ N^\top & O \end{bmatrix}$ , we may use the shorthand writing  $\begin{bmatrix} M & N \\ * & O \end{bmatrix}$  or  $\begin{bmatrix} M & * \\ N^\top & O \end{bmatrix}$ . For any matrix  $M \in \mathbb{R}^{m \times n}$ , notation  $M_{(i)}$  for  $i = 1, \dots, m$  stands for  $i$ -th row of  $M$ . A matrix  $G$  of size  $m \times n$  can also be represented as  $[g_{ij}]_{m \times n}$ , where  $g_{ij}$  denotes the  $(i, j)$ -th entry of  $G$ . For the signal  $\{h(k)\}_{k=0}^\infty$ , its  $l_\infty$  norm is defined as  $|h|_\infty := \sup_{k \geq 0} |h(k)|$ . The class  $\mathcal{K}$  and  $\mathcal{KL}$  functions are defined in the same manner as in [37, Definition 1.6, 1.9]. The function  $\text{blkdiag}(A_1, \dots, A_N)$  constructs a block diagonal matrix by placing  $A_1, \dots, A_N$  along the diagonal. We denote the ball by  $\mathcal{B}_r := \{x \in \mathbb{R}^n : |x| \leq r\}$  and the ellipsoid by  $\mathcal{E}_{M, \tau} := \{x \in \mathbb{R}^n : x^\top Mx \leq \tau\}$ .

**Definition 1.** Let  $x = 0$  be an equilibrium point of the system  $x^+ = f(x)$ . A set  $\mathcal{R} \subset \mathbb{R}^n$  is called a region of attraction (ROA) of the system relative to the equilibrium point  $x = 0$  if, for every initial state  $x(0) \in \mathcal{R}$ , the solution satisfies  $\lim_{t \rightarrow \infty} x(t) = 0$ . [37, Definition 2.28]

## II. MODEL-BASED CONTROLLER

### A. Problem Formulation

We consider the discrete-time nonlinear system with state-dependent representation

$$x^+ = A(x)x + B(x)u, \quad (1)$$

where  $x \in \mathbb{R}^n$  is the state;  $x^+$  is the forward shifting, i.e.,  $x^+(k) := x(k+1)$  for  $k \in \mathbb{N}$ ;  $u \in \mathbb{R}^m$  is the control input. For the state dependent matrices

$$A(x) = [a_{ij}(x)]_{n \times n} \quad \text{and} \quad B(x) = [b_{ij}(x)]_{n \times m}, \quad (2)$$

we assume that the entries  $a_{ij} : \mathbb{X} \mapsto \mathbb{R}$  and  $b_{ij} : \mathbb{X} \mapsto \mathbb{R}$  are continuous functions on the domain  $\mathbb{X} \subseteq \mathbb{R}^n$ , and  $\mathbb{X}$  should contain the origin  $\{0\}$ .

The problem of this section is as follows.

**Problem 1.** Design a state feedback controller  $u = Kx$  such that the origin  $x = 0$  of the closed-loop system  $x^+ = (A(x) + B(x)K)x$  is locally exponentially stable.

### B. Model-Based Controller Design

The following lemma lays the groundwork for solving Problem 1.

**Lemma 1.** *Given a positive real number  $r$ , if there exist  $P \succ 0$ ,  $\epsilon > 0$  and  $K$  such that*

$$[A(x) + B(x)K]^\top P[A(x) + B(x)K] - P \preceq -\epsilon I_n \quad (3a)$$

$$\forall x \in \mathcal{B}_r := \{x \in \mathbb{R}^n : |x| \leq r\} \subseteq \mathbb{X}, \quad (3b)$$

then there exists a region of attraction

$$\mathcal{B}_{r_0} := \{x \in \mathbb{R}^n : |x| \leq r_0\} \quad (4a)$$

where

$$r_0 = \min \left\{ r, \sqrt{\frac{\lambda_{\min}(P)}{\lambda_{\max}(P) - \epsilon}} \cdot r \right\}, \quad (4b)$$

and the closed-loop system  $x^+ = (A(x) + B(x)K)x$  starting from any  $x(0) \in \mathcal{B}_{r_0}$  will exponentially converge to the origin.

*Proof.* Let  $V(x) := x^\top Px$  and  $P \succ 0$ . For all  $x \in \mathcal{B}_r$ ,

$$\begin{aligned} V(x^+) - V(x) &= x^\top \left( [A(x) + B(x)K]^\top P[A(x) + B(x)K] - P \right) x \\ &\stackrel{(3b)}{\leq} -\epsilon |x|^2 \leq -\frac{\epsilon}{\lambda_{\max}(P)} V(x). \end{aligned}$$

The above inequalities show that (3) implies

$$V(x(k+1)) \leq \mu V(x(k)) \quad \text{with} \quad \mu := 1 - \frac{\epsilon}{\lambda_{\max}(P)} \quad (5)$$

for all  $x \in \mathcal{B}_r$ . Note that  $0 < \epsilon \leq \lambda_{\max}(P)$ , thus  $0 \leq \mu < 1$ . Next we claim that, given (5), if  $x(0) \in \mathcal{B}_{r_0}$ , then  $x(k) \in \mathcal{B}_r$  for all  $k \geq 1$ . This claim is proven in two cases.

Case (i):  $\sqrt{\lambda_{\min}(P) / (\lambda_{\max}(P) - \epsilon)} \leq 1$ . Then  $r_0 \leq r$ , and  $x(0) \in \mathcal{B}_{r_0} \subseteq \mathcal{B}_r$ . According to (5),  $V(x(1)) \leq \mu V(x(0))$ , which implies

$$\begin{aligned} |x(1)| &\leq \sqrt{\frac{\mu \lambda_{\max}(P)}{\lambda_{\min}(P)}} |x(0)| \leq \sqrt{\frac{\mu \lambda_{\max}(P)}{\lambda_{\min}(P)}} r_0 \\ &= \sqrt{\frac{\mu \lambda_{\max}(P)}{\lambda_{\min}(P)}} \sqrt{\frac{\lambda_{\min}(P)}{\lambda_{\max}(P) - \epsilon}} \cdot r = r, \end{aligned}$$

and means  $x(1) \in \mathcal{B}_r$ . Let  $x(i) \in \mathcal{B}_r$  for  $i = 1, \dots, k$ ; this condition together with (5) implies

$$\begin{aligned} V(x(k+1)) &\leq \mu^{k+1} V(x(0)) \\ \implies |x(k+1)| &\leq \mu^{\frac{k}{2}} \sqrt{\frac{\mu \lambda_{\max}(P)}{\lambda_{\min}(P)}} |x(0)| \leq \mu^{\frac{k}{2}} \cdot r < r \\ \implies x(k+1) &\in \mathcal{B}_r. \end{aligned}$$

By induction, we conclude that  $x(k) \in \mathcal{B}_r$  for all  $k \geq 1$ .

Case (ii):  $\sqrt{\lambda_{\min}(P) / (\lambda_{\max}(P) - \epsilon)} > 1$ . Then  $r_0 = r$ , and  $x(0) \in \mathcal{B}_{r_0} = \mathcal{B}_r$ . According to (5),  $V(x(1)) \leq \mu V(x(0))$ , which implies

$$|x(1)| \leq \sqrt{\frac{\mu \lambda_{\max}(P)}{\lambda_{\min}(P)}} |x(0)| \leq \sqrt{\frac{\mu \lambda_{\max}(P)}{\lambda_{\min}(P)}} \cdot r < r,$$

and means  $x(1) \in \mathcal{B}_r$ . Let  $x(i) \in \mathcal{B}_r$  for  $i = 1, \dots, k$ ; this condition together with (5) implies  $x(k+1) \in \mathcal{B}_r$  by analogous arguments as in Case (i). By induction,  $x(k) \in \mathcal{B}_r$  for all  $k \geq 1$ .

So far we conclude that, under condition (3),  $x(k) \in \mathcal{B}_r$  for all  $k \geq 0$  if  $x(0) \in \mathcal{B}_{r_0}$ . This fact implies, for all  $k \in \mathbb{N}$ ,

$$\begin{aligned} V(x(k+1)) &\leq \mu V(x(k)) \implies V(x(k)) \leq \mu^k V(x(0)) \\ \implies |x(k)| &\leq \sqrt{\lambda_{\max}(P) / \lambda_{\min}(P)} \mu^{k/2} |x(0)|, \end{aligned}$$

which completes the proof.  $\square$

It is difficult to directly solve (3), since there are infinite elements in  $\mathcal{B}_r$ . To overcome this difficulty, we use the convex polytope of  $G(x) := [A(x) \ B(x)]$  for  $x \in \mathcal{B}_r$ . Specifically, define

$$\mathcal{G} := \{G \in \mathbb{R}^{n \times (n+m)} : G = [A(x) \ B(x)], x \in \mathcal{B}_r\}. \quad (6)$$

Bearing in mind (2), let

$$\bar{a}_{ij} := \max_{x \in \mathcal{B}_r} a_{ij}(x), \quad \underline{a}_{ij} := \min_{x \in \mathcal{B}_r} a_{ij}(x), \quad (7a)$$

$$\bar{b}_{ij} := \max_{x \in \mathcal{B}_r} b_{ij}(x), \quad \underline{b}_{ij} := \min_{x \in \mathcal{B}_r} b_{ij}(x). \quad (7b)$$

Note that the maximum and minimum values exist, since  $a_{ij}(x)$  and  $b_{ij}(x)$  are assumed to be continuous on the domain  $\mathbb{X} \subseteq \mathbb{R}^n$ , and  $\mathcal{B}_r \subseteq \mathbb{X}$  is defined as a compact set. Moreover, define

$$\begin{aligned} \bar{\mathcal{G}} := \left\{ \begin{bmatrix} [\alpha_{ij}]_{n \times n} & [\beta_{ij}]_{n \times m} \end{bmatrix} \in \mathbb{R}^{n \times (n+m)} : \right. \\ \left. \alpha_{ij} \in \{\bar{a}_{ij}, \underline{a}_{ij}\}, \beta_{ij} \in \{\bar{b}_{ij}, \underline{b}_{ij}\} \right\}. \end{aligned} \quad (8)$$

The number of elements in  $\bar{\mathcal{G}}$  is finite and up to a maximum of  $2^{n \times (n+m)}$ . By the definition and property of convex hull  $\text{conv}(\cdot)$  in [42, Definition 1.5, Proposition 1.6], we have

$$\begin{aligned} \text{conv}(\bar{\mathcal{G}}) := \left\{ \begin{bmatrix} [\alpha_{ij}]_{n \times n} & [\beta_{ij}]_{n \times m} \end{bmatrix} \in \mathbb{R}^{n \times (n+m)} : \right. \\ \left. \alpha_{ij} \in [\bar{a}_{ij}, \underline{a}_{ij}], \beta_{ij} \in [\bar{b}_{ij}, \underline{b}_{ij}] \right\}. \end{aligned}$$

It is obvious that

$$\mathcal{G} \subseteq \text{conv}(\bar{\mathcal{G}}). \quad (9)$$

Now with the result of (9), we are able to give a solvable sufficient condition to (3).

**Theorem 1.** *Given a positive real number  $r$  and the set  $\mathcal{B}_r$ , if there exist  $\Gamma \succ 0$ ,  $\epsilon_\Gamma > 0$  and  $Y$  such that*

$$\begin{bmatrix} -\Gamma & G \begin{bmatrix} \Gamma \\ Y \end{bmatrix} \\ [\Gamma \ Y^\top] G^\top & -\Gamma + \epsilon_\Gamma I_n \end{bmatrix} \preceq 0 \quad \forall G \in \bar{\mathcal{G}}, \quad (10)$$

and let  $u = Kx$  with  $K = YT^{-1}$ , then there exists a region of attraction  $\mathcal{B}_{r_0}$  with

$$r_0 = \min \left\{ r, \sqrt{\frac{\lambda_{\max}(\Gamma) \lambda_{\min}(\Gamma)}{\lambda_{\max}^2(\Gamma) - \epsilon_\Gamma \lambda_{\min}(\Gamma)}} \cdot r \right\}, \quad (11)$$

and the closed-loop system  $x^+ = (A(x) + B(x)K)x$  starting from any  $x(0) \in \mathcal{B}_{r_0}$  will exponentially converge to the origin.

*Proof.* We observe that the function

$$c(G) := \begin{bmatrix} -\Gamma & G \begin{bmatrix} \Gamma \\ Y \end{bmatrix} \\ [\Gamma \ Y^\top] G^\top & -\Gamma + \epsilon_\Gamma I_n \end{bmatrix}$$

is affine and convex with respect to  $G$ . Then by [42, Proposition 1.14], (10) is equivalent to

$$\begin{aligned} c(G) \preceq 0 \quad \forall G \in \bar{\mathcal{G}} &\iff c(G) \preceq 0 \quad \forall G \in \text{conv}(\bar{\mathcal{G}}) \\ &\stackrel{(9)}{\implies} c(G) \preceq 0 \quad \forall G \in \mathcal{G}. \end{aligned}$$

In other words, bearing in mind the definition of  $\mathcal{G}$  in (6), the linear matrix inequalities (10) implies

$$\begin{bmatrix} -\Gamma & A(x)\Gamma + B(x)Y \\ \Gamma A(x)^\top + Y^\top B(x)^\top & -\Gamma + \epsilon_\Gamma I_n \end{bmatrix} \preceq 0 \quad \forall x \in \mathcal{B}_r. \quad (12)$$

Provided  $\Gamma \succ 0$ ,  $Y = K\Gamma$ , by Schur complement, the above condition is equivalent to

$$[A(x)\Gamma + B(x)K\Gamma]^\top \Gamma^{-1} [A(x)\Gamma + B(x)K\Gamma] - \Gamma \preceq -\epsilon_\Gamma I_n$$

for all  $x \in \mathcal{B}_r$ . Pre- and post-multiplying the above inequality by  $P = \Gamma^{-1}$  leads to

$$\begin{aligned} [A(x) + B(x)K]^\top P [A(x) + B(x)K] - P &\preceq -\epsilon_\Gamma P^2 \\ &\preceq -\epsilon_\Gamma \lambda_{\min}^2(P) I_n \preceq -\frac{\epsilon_\Gamma}{\lambda_{\max}^2(\Gamma)} I_n, \end{aligned}$$

which implies

$$[A(x) + B(x)K]^\top P [A(x) + B(x)K] - P \preceq -\epsilon I_n \quad \forall x \in \mathcal{B}_r$$

with  $\epsilon = \epsilon_\Gamma / \lambda_{\max}^2(\Gamma) > 0$ , that is, (3) in Lemma 1 holds. As for the region of attraction  $\mathcal{B}_{r_0}$ , (4b) rewrites into (11) through  $\lambda_{\max}(P) = \lambda_{\min}^{-1}(\Gamma)$  and  $\lambda_{\min}(P) = \lambda_{\max}^{-1}(\Gamma)$ . This completes the proof.  $\square$

**Example 1.** Consider the nonlinear system

$$\begin{cases} x_1^+ = x_1 + 0.1 \sin x_1 + 0.2 x_2 + (0.1 + 0.1|x_2|)u \\ x_2^+ = 0.2 x_1 + 0.9 x_2 + 0.1 x_1^2 x_2 + 0.1 e^{x_1} u \end{cases} \quad (13)$$

with the corresponding state-dependent representation

$$A(x) = \begin{bmatrix} 1 + 0.1 \frac{\sin x_1}{x_1} & 0.2 \\ 0.2 & 0.9 + 0.1 x_1^2 \end{bmatrix}, \quad B(x) = \begin{bmatrix} 0.1 + 0.1|x_2| \\ 0.1 e^{x_1} \end{bmatrix}.$$

Take  $r = 1.1$  for  $\mathcal{B}_r$ . In (7),  $\bar{a}_{11} := \max_{x \in \mathcal{B}_r} a_{11}(x) = 1.1$ ,  $\underline{a}_{11} := \min_{x \in \mathcal{B}_r} a_{11}(x) = 1.081$ ,  $\bar{a}_{21} = \underline{a}_{21} = 0.2$ ,  $\bar{a}_{12} = \underline{a}_{12} = 0.2$ ,  $\bar{a}_{22} = 1.021$ ,  $a_{22} = 0.9$ ,  $\bar{b}_{11} = 0.21$ ,  $\underline{b}_{11} = 0.1$ ,  $\bar{b}_{21} = 0.3004$ ,  $\underline{b}_{21} = 0.0332$ , which lead to the set  $\bar{\mathcal{G}}$  as in (8). By Theorem 1, solving (10) via CVX [43] yields  $\epsilon_\Gamma = 0.1402$ ,  $Y = [-65.0340 \ -78.9831]$ ,  $\Gamma = \begin{bmatrix} 34.3888 & 0.0000 \\ 0.0000 & 34.3888 \end{bmatrix}$ , and  $K = [-1.8911 \ -2.2968]$ . According to (11), the estimate of ROA,  $\mathcal{B}_{r_0}$ , has a radius of  $r_0 = 1.1$ . Figure 1 is the phase portrait of the closed-loop system  $x^+ = A(x)x + B(x)Kx$ .  $\diamond$

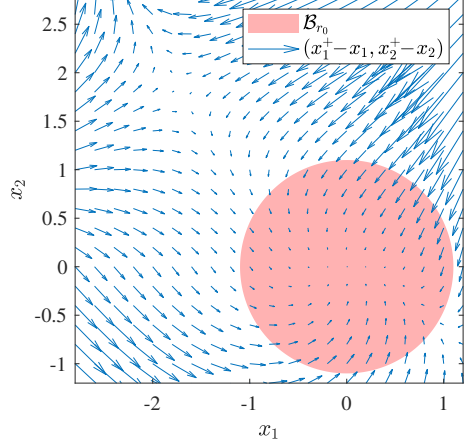


Fig. 1. Phase portrait of the closed-loop system with model-based controller.

### C. Robustness Against Disturbances

In this subsection, we explore the robustness of the controller against disturbances. To be specific, during the controller implementation, we consider the following closed-loop model

$$x^+ = (A(x) + B(x)K)x + w \quad (14)$$

where  $K$  is solved from LMIs (10) and  $w \in \mathbb{R}^n$  is the disturbance. It is proved in Theorem 1 that, without disturbance ( $w = 0$ ), the closed-loop system is exponentially stable if initial state  $x(0) \in \mathcal{B}_{r_0}$ . While under the influence of the disturbance  $w$ , the system exhibits a property similar to the input-to-state stability [38], which is established in the next theorem.

**Theorem 2.** For the disturbed closed-loop system (14), given a positive real number  $r$  and the set  $\mathcal{B}_r$ , suppose that there exist  $\Gamma \succ 0$ ,  $\epsilon_\Gamma > 0$  and  $Y$  such that (10) holds, and let  $K = Y\Gamma^{-1}$  for (14). If the initial state  $x(0)$  and disturbance  $w(k)$  satisfy

$$|x(0)|^2 \leq r^2 \quad \text{and} \quad \delta_{x_0}|x(0)|^2 + \delta_w|w|_\infty^2 \leq r^2, \quad (15a)$$

where

$$\delta_{x_0} := \frac{2\lambda_{\max}^2(\Gamma) - \epsilon_\Gamma \lambda_{\min}(\Gamma)}{2\lambda_{\min}(\Gamma)\lambda_{\max}(\Gamma)}, \quad (15b)$$

$$\delta_w := \frac{4\gamma_{A_{\text{cl}}}^2 \lambda_{\max}^5(\Gamma) + 2\epsilon_\Gamma \lambda_{\min}(\Gamma)\lambda_{\max}^3(\Gamma)}{\epsilon_\Gamma^2 \lambda_{\min}^3(\Gamma)}, \quad (15c)$$

$$\gamma_{A_{\text{cl}}} := \max_{x \in \mathcal{B}_r} \|A(x) + B(x)K\|, \quad (15d)$$

then there exists  $\beta \in \mathcal{KL}$  and  $\gamma \in \mathcal{K}$  such that

$$|x(k)| \leq \beta(x(0), k) + \gamma(|w|_\infty) \quad \forall k \in \mathbb{N}. \quad (16)$$

*Proof.* In Theorem 1 we have proven that if there exist  $\Gamma \succ 0$ ,  $\epsilon_\Gamma > 0$  and  $Y$  such that (10) holds, then

$$[*]^\top P \cdot [A(x) + B(x)K] - P \preceq -\epsilon I_n \quad \forall x \in \mathcal{B}_r \quad (17)$$

with  $K = Y\Gamma^{-1}$ ,  $P = \Gamma^{-1}$  and  $\epsilon = \epsilon_\Gamma / \lambda_{\max}^2(\Gamma) > 0$ . Let  $V(x) := x^\top P x$  and  $A_{\text{cl}} := A(x) + B(x)K$ . Along with the trajectory of (14),

$$V(x(k+1)) - V(x(k)) = V(A_{\text{cl}}x(k)) - V(x(k))$$

$$\begin{aligned}
& + V(A_{\text{cl}}x(k) + w(k)) - V(A_{\text{cl}}x(k)) \\
= & x(k)^\top (A_{\text{cl}}^\top P A_{\text{cl}} - P)x(k) \\
& + 2x(k)^\top A_{\text{cl}}^\top P w(k) + w(k)^\top P w(k) \\
\stackrel{(17)}{\leq} & -\epsilon |x(k)|^2 + 2x(k)^\top A_{\text{cl}}^\top P w(k) + w(k)^\top P w(k) \quad (18)
\end{aligned}$$

for all  $x(k) \in \mathcal{B}_r$ . Let  $\gamma_{A_{\text{cl}}} := \max_{x \in \mathcal{B}_r} \|A(x) + B(x)K\|$  and  $|w|_\infty := \sup_{k \geq 0} |w(k)|$ , then

$$\begin{aligned}
(18) \leq & -\epsilon |x(k)|^2 \\
& + 2\gamma_{A_{\text{cl}}} \lambda_{\max}(P) |x(k)| |w|_\infty + \lambda_{\max}(P) |w|_\infty^2. \quad (19)
\end{aligned}$$

For any  $\alpha > 0$ , the Young's inequality yields

$$2|x(k)| |w|_\infty \leq \frac{1}{\alpha} |x(k)|^2 + \alpha |w|_\infty^2.$$

By taking  $\alpha := 2\gamma_{A_{\text{cl}}} \lambda_{\max}(P)/\epsilon$ , we have

$$\begin{aligned}
(19) \leq & -\frac{\epsilon}{2} |x(k)|^2 \\
& + \underbrace{\left(2\gamma_{A_{\text{cl}}}^2 \lambda_{\max}^2(P)/\epsilon + \lambda_{\max}(P)\right) |w|_\infty^2}_{=: c_w}. \quad (20)
\end{aligned}$$

For all  $x(k) \in \mathcal{B}_r$ , combining (18), (19) and (20) gives

$$\begin{aligned}
V(x(k+1)) - V(x(k)) & \leq -\frac{\epsilon}{2\lambda_{\max}(P)} V(x(k)) + c_w |w|_\infty^2 \\
\iff V(x(k+1)) & \leq \mu_w V(x(k)) + c_w |w|_\infty^2 \quad (21a)
\end{aligned}$$

where

$$\mu_w := 1 - \frac{\epsilon}{2\lambda_{\max}(P)}. \quad (21b)$$

Note that  $0 < \epsilon \leq \lambda_{\max}(P)$ , thus  $0 < \mu_w < 1$ . Moreover, note that (21) only holds for  $x(k) \in \mathcal{B}_r$ . Next we need to prove that, if (15) holds, then (21) holds for all  $k \in \mathbb{N}$ . Bearing in mind  $\lambda_{\max}(P) = \lambda_{\min}^{-1}(\Gamma)$ ,  $\lambda_{\min}(P) = \lambda_{\max}^{-1}(\Gamma)$  and  $\epsilon = \epsilon_\Gamma/\lambda_{\max}^2(\Gamma)$ , (15) equivalently rewrites as  $|x(0)|^2 \leq r^2$  and

$$\frac{\lambda_{\max}(P)}{\lambda_{\min}(P)} \mu_w |x(0)|^2 + \frac{1}{1 - \mu_w} \frac{c_w}{\lambda_{\min}(P)} |w|_\infty^2 \leq r^2. \quad (22)$$

For  $x(0) \in \mathcal{B}_r$ , (21) holds at  $k = 0$ , which implies

$$|x(1)|^2 \leq \frac{\lambda_{\max}(P)}{\lambda_{\min}(P)} \mu_w |x(0)|^2 + \frac{c_w}{\lambda_{\min}(P)} |w|_\infty^2 \stackrel{(22)}{\leq} r^2,$$

and further implies  $x(1) \in \mathcal{B}_r$ . Let  $x(i) \in \mathcal{B}_r$  for  $i = 1, \dots, k$ ; this condition together with (21) implies

$$\begin{aligned}
V(x(k+1)) & \leq \mu_w^{k+1} V(x(0)) \\
& + (1 + \mu_w + \dots + \mu_w^k) c_w |w|_\infty^2 \\
\implies |x(k+1)|^2 & \leq \frac{\lambda_{\max}(P)}{\lambda_{\min}(P)} \mu_w^{k+1} |x(0)|^2 \\
& + \frac{1 - \mu_w^{k+1}}{1 - \mu_w} \frac{c_w}{\lambda_{\min}(P)} |w|_\infty^2 \\
\stackrel{(22)}{\leq} & |x(k+1)|^2 \leq r^2 \implies x(k+1) \in \mathcal{B}_r
\end{aligned}$$

By induction,  $x(k) \in \mathcal{B}_r$  for all  $k \geq 1$ . So far we conclude that suppose (10) is feasible, if (15) holds, then (21) holds for all  $k \in \mathbb{N}$ , and

$$|x(k)|^2 \leq \frac{\lambda_{\max}(P)}{\lambda_{\min}(P)} \mu_w^k |x(0)|^2 + \frac{1}{1 - \mu_w} \frac{c_w}{\lambda_{\min}(P)} |w|_\infty^2$$

for all  $k \in \mathbb{N}$ , that is, (16) holds. This completes the proof.  $\square$

**Example 2.** Following Example 1, the controller  $K$  remains unchanged. For the closed-loop system  $x^+ = (A(x) + B(x)K)x + w$ , we set  $x(0) = (-0.5, -0.5)$  and the disturbance  $(w_1, w_2)$  as random variables uniformly distributed in the interval  $[-0.1, 0.1]$ . The simulation result is depicted in Figure 2, which is consistent with (16) in Theorem 2.  $\triangleleft$

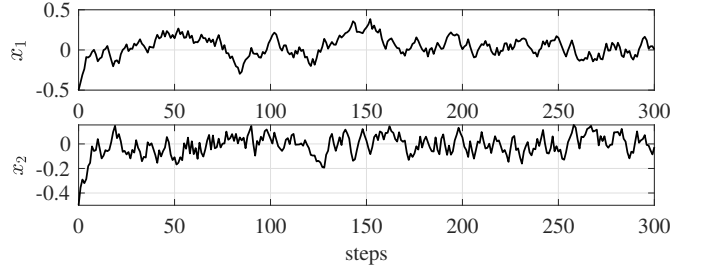


Fig. 2. State response of the closed-loop system with model-based controller under disturbance.

#### D. System Subject to Input Saturation

In this subsection, we consider the system subject to input saturation:

$$x^+ = A(x)x + B(x) \text{sat}(u). \quad (23)$$

The saturation function  $\text{sat}(u)$  maps from  $\mathbb{R}^m$  to  $\mathbb{R}^m$  with its components defined as

$$\text{sat}(u_i) := \text{sign}(u_i) \min(|u_i|, \bar{u}_i) \quad \text{for } i = 1, \dots, m, \quad (24)$$

where  $u_i$  is the  $i$ -th control input, and  $\bar{u}_i > 0$  is the  $i$ -th entry of  $\bar{u}$  that is the level vector of the saturation.

Given the control law  $u = Kx$ , the closed-loop system subject to input saturation is

$$x^+ = (A(x)x + B(x)\phi(Kx)), \quad (25)$$

where  $\phi(u)$  is the dead-zone function defined as

$$\phi(u) := \text{sat}(u) - u. \quad (26)$$

Referring to [39, Lemma 1.6] and [44, Lemma 1], the generalized sector condition lemma, as stated below, is used to handle the dead-zone (26).

**Lemma 2.** Given a matrix  $L \in \mathbb{R}^{m \times n}$ , for every  $x \in \mathcal{S}(L)$  where

$$\mathcal{S}(L) := \{x \in \mathbb{R}^n : |L_{(i)}x| \leq \bar{u}_i, \forall i = 1, \dots, m\}, \quad (27)$$

the following relation holds:

$$\phi(u)^\top N(\text{sat}(u) + Lx) \leq 0 \quad (28)$$

with any diagonal positive definite matrix  $N \in \mathbb{R}^{m \times m}$ .

Before going to the main result, we need the following intermediate lemma.

**Lemma 3.** Given a positive real number  $r$  and the set  $\mathcal{B}_r$ , if there exist  $P \succ 0$ ,  $\tau > 0$ ,  $\epsilon > 0$ , and  $V(x) := x^\top Px$ , such that

$$V(x^+) - V(x) \leq -\epsilon |x|^2 \quad \forall x \in \mathcal{B}_r \cap \mathcal{E}_{P, \tau}, \quad (29)$$

then there exists a region of attraction  $\mathcal{B}_{r_0} \cap \mathcal{E}_{P,\tau}$  with

$$r_0 = \min \left\{ r, \sqrt{\frac{\lambda_{\min}(P)}{\lambda_{\max}(P) - \epsilon}} \cdot r \right\}, \quad (30)$$

and the closed-loop system  $x^+ = A(x)x + B(x)\text{sat}(Kx)$  starting from any  $x(0) \in \mathcal{B}_{r_0} \cap \mathcal{E}_{P,\tau}$  will exponentially converge to the origin.

*Proof.* The condition (29) implies that, for  $x(k) \in \mathcal{B}_r \cap \mathcal{E}_{P,\tau}$ ,

$$V(x(k+1)) \leq \mu V(x(k)) \quad \text{with } \mu := 1 - \frac{\epsilon}{\lambda_{\max}(P)}, \quad (31)$$

which corresponds to (5). Using analogous arguments as in the proof of Lemma 1, we obtain that  $x(k) \in \mathcal{B}_r$  for all  $k \geq 1$  if  $x(0) \in \mathcal{B}_{r_0}$  with  $r_0$  specified in (30), which is consistent with (4b). Moreover, for any  $x(k) \in \mathcal{E}_{P,\tau}$ ,

$$\begin{aligned} x(k) \in \mathcal{E}_{P,\tau} &\stackrel{0 \leq \mu}{\iff} \mu V(x(k)) \leq \mu \tau \stackrel{(31)}{\iff} V(x(k+1)) \leq \mu \tau \\ &\stackrel{0 \leq \mu \leq 1}{\iff} V(x(k+1)) \leq \tau \iff x(k+1) \in \mathcal{E}_{P,\tau}. \end{aligned}$$

In other words,  $x(k) \in \mathcal{E}_{P,\tau}$  for all  $k \geq 1$  if  $x(0) \in \mathcal{E}_{P,\tau}$ . So far we conclude that, under condition (31), if  $x(0) \in \mathcal{B}_{r_0} \cap \mathcal{E}_{P,\tau}$ , then  $x(k) \in \mathcal{B}_r \cap \mathcal{E}_{P,\tau}$  for all  $k \geq 1$ . This fact implies that

$$V(x(k+1)) \leq \mu V(x(k)) \quad \forall k \geq 0,$$

with  $0 \leq \mu < 1$ , which completes the proof.  $\square$

The main result of this subsection is given below.

**Theorem 3.** Given a positive real number  $r$  and the set  $\mathcal{B}_r$ , if there exist  $\Gamma \succ 0$ ,  $\epsilon_\Gamma > 0$ ,  $Y$ ,  $W$  and diagonal positive definite matrix  $S$  such that

$$\begin{bmatrix} \Gamma & W_{(i)}^\top \\ W_{(i)} & \bar{u}_i^2 \end{bmatrix} \succeq 0 \quad i = 1, \dots, m, \quad (32a)$$

$$\begin{bmatrix} -\Gamma + \epsilon_\Gamma I_n & -Y^\top - W^\top & \begin{bmatrix} \Gamma \\ Y \end{bmatrix}^\top G^\top \\ -Y - W & -2S & \begin{bmatrix} 0 \\ S \end{bmatrix}^\top G^\top \\ G \begin{bmatrix} \Gamma \\ Y \end{bmatrix} & G \begin{bmatrix} 0 \\ S \end{bmatrix} & -\Gamma \end{bmatrix} \preceq 0 \quad \forall G \in \bar{\mathcal{G}}, \quad (32b)$$

and let  $u = Kx$  with  $K = Y\Gamma^{-1}$ , then there exists a region of attraction  $\mathcal{B}_{r_0} \cap \mathcal{E}_{P,1}$  with  $P = \Gamma^{-1}$  and

$$r_0 = \min \left\{ r, \sqrt{\frac{\lambda_{\max}(\Gamma)\lambda_{\min}(\Gamma)}{\lambda_{\max}^2(\Gamma) - \epsilon_\Gamma\lambda_{\min}(\Gamma)}} \cdot r \right\}, \quad (33)$$

and the closed-loop system  $x^+ = A(x)x + B(x)\text{sat}(Kx)$  starting from any  $x(0) \in \mathcal{B}_{r_0} \cap \mathcal{E}_{P,1}$  will exponentially converge to the origin.

*Proof.* Pre- and post-multiplying the inequalities in (32a) by  $\text{blkdiag}(\Gamma^{-1}, 1)$  yields, with  $L = WT\Gamma^{-1}$ ,

$$\begin{bmatrix} \Gamma^{-1} & L_{(i)}^\top \\ L_{(i)} & \bar{u}_i^2 \end{bmatrix} \succeq 0 \Leftrightarrow L_{(i)}\Gamma L_{(i)}^\top \leq \bar{u}_i^2 \Leftrightarrow |L_{(i)}\Gamma^{1/2}| \leq \bar{u}_i.$$

For every  $x \in \mathcal{E}_{P,1}$ , we have  $|P^{1/2}x| \leq 1$  and

$$|L_{(i)}x| = |L_{(i)}\Gamma^{1/2}P^{1/2}x| \leq |L_{(i)}\Gamma^{1/2}| \cdot |P^{1/2}x| = \bar{u}_i,$$

which implies  $x \in \mathcal{S}(L)$ , namely,  $\mathcal{E}_{P,1} \subseteq \mathcal{S}(L)$ . By Lemma 2, we conclude that (32a) results in

$$\phi(u)^\top N(\text{sat}(u) + Lx) \leq 0 \quad \forall x \in \mathcal{E}_{P,1} \quad (34)$$

with any diagonal positive definite matrix  $N$ .

Define the function

$$c(G) := \begin{bmatrix} -\Gamma + \epsilon_\Gamma I_n & * & * \\ -Y - W & -2S & * \\ G \begin{bmatrix} \Gamma \\ Y \end{bmatrix} & G \begin{bmatrix} 0 \\ S \end{bmatrix} & -\Gamma \end{bmatrix}.$$

Condition (32b) is equivalent to

$$\begin{aligned} c(G) \preceq 0 \quad \forall G \in \bar{\mathcal{G}} &\iff c(G) \preceq 0 \quad \forall G \in \text{conv}(\bar{\mathcal{G}}) \\ &\stackrel{(9)}{\iff} c(G) \preceq 0 \quad \forall G \in \mathcal{G} \\ &\stackrel{(6)}{\iff} c([A(x) \ B(x)]) \preceq 0 \quad \forall x \in \mathcal{B}_r. \end{aligned}$$

Taking  $W = L\Gamma$ ,  $N = S^{-1}$ ,  $Y = K\Gamma$ , pre- and post-multiplying  $c([A(x) \ B(x)])$  by  $\text{blkdiag}(I_n, N, I_n)$  results in

$$\begin{bmatrix} -\Gamma + \epsilon_\Gamma I_n & * & * \\ -N(K\Gamma + L\Gamma) & -2N & * \\ A(x)\Gamma + B(x)K\Gamma & B(x) & -\Gamma \end{bmatrix} \preceq 0 \quad \forall x \in \mathcal{B}_r.$$

Let  $\epsilon = \epsilon_\Gamma/\lambda_{\max}^2(\Gamma)$ , the above inequality implies

$$\begin{bmatrix} -\Gamma + \epsilon\Gamma^2 & * & * \\ -N(K\Gamma + L\Gamma) & -2N & * \\ A(x)\Gamma + B(x)K\Gamma & B(x) & -\Gamma \end{bmatrix} \preceq 0 \quad \forall x \in \mathcal{B}_r.$$

Pre- and post-multiplying both sides of the above inequality by  $\text{blkdiag}(P, I_m, I_n)$  with  $P = \Gamma^{-1}$ , and by Schur complement, the above inequality is equivalent to  $H(x) \preceq 0$  for all  $x \in \mathcal{B}_r$ , where

$$\begin{aligned} H(x) := & \quad (35) \\ & \begin{bmatrix} (A(x) + B(x)K)^\top P(A(x) + B(x)K) - P + \epsilon I_n \\ B(x)^\top P(A(x) + B(x)K) - N(K + L) \\ (A(x) + B(x)K)^\top PB(x) - (K + L)^\top N \\ B(x)^\top PB(x) - 2N \end{bmatrix}. \end{aligned}$$

This fact implies, for  $V(x) := x^\top Px$ ,

$$\begin{aligned} & \begin{bmatrix} x \\ \phi(Kx) \end{bmatrix}^\top H(x) \begin{bmatrix} x \\ \phi(Kx) \end{bmatrix} \leq 0 \quad \forall x \in \mathcal{B}_r \\ & \stackrel{(25),(28)}{\iff} V(x^+) - V(x) \\ & \quad - 2\phi(Kx)^\top N(\text{sat}(Kx) + Lx) \leq -\epsilon|x|^2 \quad \forall x \in \mathcal{B}_r. \end{aligned}$$

Because of (32a) and (34), we obtain

$$V(x^+) - V(x) \leq -\epsilon|x|^2 \quad \forall x \in \mathcal{B}_r \cap \mathcal{E}_{P,1},$$

which is consistent with (29). Then by Lemma 3, and rewriting (30) to (33) via  $\epsilon = \epsilon_\Gamma/\lambda_{\max}^2(\Gamma)$ ,  $\lambda_{\max}(P) = \lambda_{\min}^{-1}(\Gamma)$  and  $\lambda_{\min}(P) = \lambda_{\max}^{-1}(\Gamma)$ , we complete the proof.  $\square$

**Example 3.** Consider the system (13) as in Example 1. Take  $r = 1.1$  for  $\mathcal{B}_r$ . By (7), we have the set  $\bar{\mathcal{G}}$  as in (8). For different level of the saturation  $\bar{u} \in \{4.0, 2.0, 1.0, 0.5\}$ , solving (32) in Theorem 3 via CVX yields  $K = [-1.8155 - 2.3147, -1.8155 - 2.3146, -1.8155 - 2.3147]$  and

$[-1.9241 - 2.3214]$ , respectively. Note that the program (32) in Theorem 3 is only a feasibility problem, hence we set minimizing  $[\lambda_{\max}(\Gamma) - \lambda_{\min}(\Gamma) - \epsilon_{\Gamma} - 0.1\text{trace}(\Gamma)]$  as the objective when solving the LMIs (32). The estimate of ROA,  $\mathcal{B}_{r_0} \cap \mathcal{E}_{P,1}$ , for different values of  $\bar{u}$  is shown in Figure 3.  $\triangleleft$

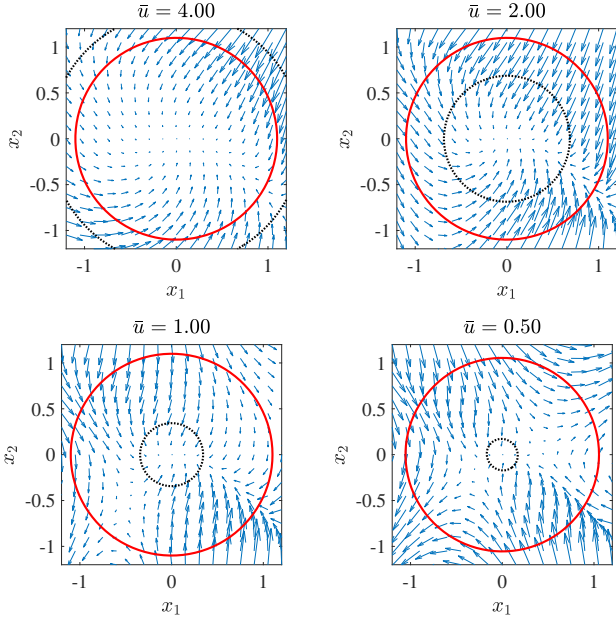


Fig. 3. Estimate of ROA,  $\mathcal{B}_{r_0} \cap \mathcal{E}_{P,1}$ , for different saturation levels. The red solid ball is  $\mathcal{B}_{r_0}$ ; the black dashed ellipsoid is  $\mathcal{E}_{P,1}$ ; the background is the phase portrait regarding the closed-loop system  $x^+ = A(x)x + B(x)\text{sat}(Kx)$ .

### III. DATA-DRIVEN CONTROLLER

#### A. Problem Formulation

In this section, for the system (1), while the state matrix  $A(x)$  and input matrix  $B(x)$  are assumed to be unknown, we assume the existence of a known function library that can construct  $A(x)$  and  $B(x)$ , as stated in the following assumption.

**Assumption 1.** Condition (i) and (ii) below holds.

(i) For each  $j = 1, \dots, n$ , we know a vector-valued function  $\xi_{A_j} : \mathbb{R}^n \mapsto \mathbb{R}^{n \times n_{A_j}}$  which is continuous on the domain  $\mathbb{X} \subseteq \mathbb{R}^n$ , such that

$$(a_{1j}(x), \dots, a_{ij}(x), \dots, a_{nj}(x)) = E_{A_j} \xi_{A_j}(x) \quad (36)$$

for some constant matrix  $E_{A_j} \in \mathbb{R}^{n \times n_{A_j}}$ .

(ii) For each  $j = 1, \dots, m$ , we know a vector-valued function  $\xi_{B_j} : \mathbb{R}^n \mapsto \mathbb{R}^{n \times n_{B_j}}$  which is continuous on the domain  $\mathbb{X} \subseteq \mathbb{R}^n$ , such that

$$(b_{1j}(x), \dots, b_{ij}(x), \dots, b_{nj}(x)) = E_{B_j} \xi_{B_j}(x) \quad (37)$$

for some constant matrix  $E_{B_j} \in \mathbb{R}^{n \times n_{B_j}}$ .

Assumption 1 allows us to rewrite the system (1) as

$$\begin{aligned} x^+ &= A(x)x + B(x)u \\ &= [E_{A_1} \xi_{A_1}(x) \dots E_{A_n} \xi_{A_n}(x)]x \\ &\quad + [E_{B_1} \xi_{B_1}(x) \dots E_{B_m} \xi_{B_m}(x)]u \end{aligned}$$

$$= E_A \Xi_A(x)x + E_B \Xi_B(x)u \quad (38a)$$

where

$$E_A := [E_{A_1} \dots E_{A_n}] \in \mathbb{R}^{n \times n_A}, \quad n_A := \sum_{j=1}^n n_{A_j}, \quad (38b)$$

$$\Xi_A(x) := \text{blkdiag}(\xi_{A_1}(x), \dots, \xi_{A_n}(x)), \quad (38c)$$

$$E_B := [E_{B_1} \dots E_{B_m}] \in \mathbb{R}^{n \times n_B}, \quad n_B := \sum_{j=1}^m n_{B_j}, \quad (38d)$$

$$\Xi_B(x) := \text{blkdiag}(\xi_{B_1}(x), \dots, \xi_{B_m}(x)). \quad (38e)$$

Note that  $(\Xi_A(x), \Xi_B(x))$  are known by Assumption 1 and  $(E_A, E_B)$  are unknown. The deficiency of model knowledge is compensated by the data collected from experiments.

During the experiment, we consider that the system (38) is affected by process noise  $d \in \mathbb{R}^n$ , i.e.,

$$x_d^+ = E_A \Xi_A(x_d)x_d + E_B \Xi_B(x_d)u_d + d. \quad (39)$$

The experimental input data is  $\{u_d(k)\}_{k=0}^{T-1}$  and the corresponding state data is  $\{x_d(k)\}_{k=0}^T$ , where  $T > 0$  is the number of samples.

The problem of this section is summarized as follows.

**Problem 2.** Without the model knowledge  $(E_A, E_B)$ , using the experimental data  $\{u_d(k)\}_{k=0}^{T-1}$  and  $\{x_d(k)\}_{k=0}^T$ , design a state feedback controller  $u = Kx$  such that the origin  $x = 0$  of the closed-loop system  $x^+ = (A(x) + B(x)K)x$  is locally exponentially stable.

#### B. Data-Driven Controller Design

We first arrange the data as the following matrices

$$X_0 := [\Xi_A(x_d(0))x_d(0) \dots \Xi_A(x_d(T-1))x_d(T-1)], \quad (40a)$$

$$X_1 := [x_d(1) \dots x_d(T)], \quad (40b)$$

$$U_0 := [\Xi_B(x_d(0))u_d(0) \dots \Xi_B(x_d(T-1))u_d(T-1)], \quad (40c)$$

and arrange the unknown noise as

$$D_0 := [d(0) \dots d(T-1)]. \quad (40d)$$

According to (39), the above data matrices satisfy

$$X_1 = E_A X_0 + E_B U_0 + D_0. \quad (41)$$

For further analysis, we assume that the noise sequence  $D_0$  has bounded energy, which is described in the following assumption.

**Assumption 2.** The energy bound  $\Theta \succeq 0$  is known, and

$$D_0 \in \mathcal{D} := \{D \in \mathbb{R}^{n \times T} : DD^\top \preceq \Theta\}. \quad (42)$$

Although the model knowledge of  $E_A$  and  $E_B$  is absent, Assumption 2 enables us to characterize the set of all possible pairs  $(\hat{E}_A, \hat{E}_B)$  that can generate data  $\{u_d(k)\}_{k=0}^{T-1}$  and  $\{x_d(k)\}_{k=0}^T$  while keeping the noise sequence in the set  $\mathcal{D}$ , namely,

$$\begin{aligned} \mathcal{C} &:= \left\{ [\hat{E}_A \hat{E}_B] : X_1 = \hat{E}_A X_0 + \hat{E}_B U_0 + D, D \in \mathcal{D} \right\} \\ &= \left\{ [\hat{E}_A \hat{E}_B] : X_1 = \hat{E}_A X_0 + \hat{E}_B U_0 + D, DD^\top \preceq \Theta \right\} \end{aligned}$$

$$\begin{aligned}
&= \left\{ [\hat{E}_A \hat{E}_B] : \left[ X_1 - \hat{E}_A X_0 - \hat{E}_B U_0 \right] \cdot \left[ * \right]^\top \preceq \Theta \right\} \\
&= \left\{ Z = [\hat{E}_A \hat{E}_B] : ZAZ^\top + ZB^\top + BZ^\top + C \preceq 0 \right\} \quad (43a)
\end{aligned}$$

with

$$\mathbf{A} := \begin{bmatrix} X_0 \\ U_0 \end{bmatrix} \begin{bmatrix} X_0 \\ U_0 \end{bmatrix}^\top, \quad \mathbf{B} := -X_1 \begin{bmatrix} X_0 \\ U_0 \end{bmatrix}^\top, \quad (43b)$$

$$\mathbf{C} := X_1 X_1^\top - \Theta. \quad (43c)$$

We make the next assumption on data.

**Assumption 3.** Data matrix  $\begin{bmatrix} X_0 \\ U_0 \end{bmatrix}$  has full row rank.

By Assumption 3 and [15, Proposition 1], the set  $\mathcal{C}$  equivalently rewrites as

$$\mathcal{C} = \left\{ \mathbf{Z}_c + \mathbf{Q}^{1/2} \Upsilon \mathbf{A}^{-1/2} : \Upsilon \Upsilon^\top \preceq I_n \right\}, \quad (44a)$$

$$\mathbf{Z}_c := -\mathbf{B} \mathbf{A}^{-1}, \quad \mathbf{Q} := \mathbf{B} \mathbf{A}^{-1} \mathbf{B}^\top - \mathbf{C}. \quad (44b)$$

Lemma 1 in the model-based case presents a groundwork to Problem 1, which in turn informs our approach to solving Problem 2, that is, finding  $P \succ 0$ ,  $\epsilon > 0$  and  $K$  such that

$$[*]^\top P \cdot [\hat{E}_A \Xi_A(x) + \hat{E}_B \Xi_B(x) K] - P \preceq -\epsilon I_n \quad (45a)$$

$$\forall x \in \mathcal{B}_r := \{x \in \mathbb{R}^n : |x| \leq r\} \text{ and } \forall (\hat{E}_A, \hat{E}_B) \in \mathcal{C}. \quad (45b)$$

However, in (45b), there are infinite elements in  $\mathcal{B}_r$  and  $\mathcal{C}$ . To overcome these challenges, we first use the convex polytope of  $Q(x) := \text{blkdiag}(\Xi_A(x), \Xi_B(x))$  for  $x \in \mathcal{B}_r$ , and then apply Petersen's lemma [15] to handle  $\mathcal{C}$ .

Similar to (6), we introduce

$$\begin{aligned}
\mathcal{Q} := \left\{ Q \in \mathbb{R}^{(n_A+n_B) \times (n+m)} : \right. \\
\left. Q(x) = \text{blkdiag}(\Xi_A(x), \Xi_B(x)), \quad x \in \mathcal{B}_r \right\}. \quad (46)
\end{aligned}$$

Bearing in mind Assumption 1, the entries of  $\xi_{A_j}$  for  $j = 1, \dots, n$  are given by

$$(\xi_{1j}^A, \dots, \xi_{ij}^A, \dots, \xi_{n_{A_j}j}^A) := \xi_{A_j};$$

the entries of  $\xi_{B_j}$  for  $j = 1, \dots, m$  are given by

$$(\xi_{1j}^B, \dots, \xi_{ij}^B, \dots, \xi_{n_{B_j}j}^B) := \xi_{B_j}.$$

Let

$$\bar{\xi}_{ij}^A := \max_{x \in \mathcal{B}_r} \xi_{ij}^A(x), \quad \underline{\xi}_{ij}^A := \min_{x \in \mathcal{B}_r} \xi_{ij}^A(x), \quad (47a)$$

$$\bar{\xi}_{ij}^B := \max_{x \in \mathcal{B}_r} \xi_{ij}^B(x), \quad \underline{\xi}_{ij}^B := \min_{x \in \mathcal{B}_r} \xi_{ij}^B(x). \quad (47b)$$

Note that the maximum and minimum values exist, since  $\xi_{A_j}(x)$  and  $\xi_{B_j}(x)$  are continuous by Assumption 1. Moreover, define

$$\bar{\mathcal{Q}} := \left\{ \text{blkdiag}(\zeta_{A_1}, \dots, \zeta_{A_n}, \zeta_{B_1}, \dots, \zeta_{B_m}) : \right. \quad (48)$$

$$\zeta_{A_j} := (\zeta_{1j}^A, \dots, \zeta_{ij}^A, \dots, \zeta_{n_{A_j}j}^A), \quad \zeta_{ij}^A \in \{\bar{\xi}_{ij}^A, \underline{\xi}_{ij}^A\}$$

$$\zeta_{B_j} := (\zeta_{1j}^B, \dots, \zeta_{ij}^B, \dots, \zeta_{n_{B_j}j}^B), \quad \zeta_{ij}^B \in \{\bar{\xi}_{ij}^B, \underline{\xi}_{ij}^B\}.$$

The number of elements in  $\bar{\mathcal{Q}}$  is finite and up to a maximum of  $2^{n_A+n_B}$ . By the definition and property of convex hull, we have

$$\begin{aligned}
\text{conv}(\bar{\mathcal{Q}}) := \left\{ \text{blkdiag}(\zeta_{A_1}, \dots, \zeta_{A_n}, \zeta_{B_1}, \dots, \zeta_{B_m}) : \right. \\
\zeta_{A_j} := (\zeta_{1j}^A, \dots, \zeta_{ij}^A, \dots, \zeta_{n_{A_j}j}^A), \quad \zeta_{ij}^A \in [\bar{\xi}_{ij}^A, \underline{\xi}_{ij}^A] \\
\zeta_{B_j} := (\zeta_{1j}^B, \dots, \zeta_{ij}^B, \dots, \zeta_{n_{B_j}j}^B), \quad \zeta_{ij}^B \in [\bar{\xi}_{ij}^B, \underline{\xi}_{ij}^B] \left. \right\}.
\end{aligned}$$

It is obvious that

$$\mathcal{Q} \subseteq \text{conv}(\bar{\mathcal{Q}}). \quad (49)$$

Analogous to Theorem 1, we have the next result.

**Lemma 4.** Under Assumption 1 and 2, given a positive real number  $r$  and the set  $\mathcal{B}_r$ , if there exist  $\Gamma \succ 0$ ,  $\epsilon_\Gamma > 0$  and  $Y$  such that

$$\begin{bmatrix} -\Gamma & [\hat{E}_A \hat{E}_B] Q \begin{bmatrix} \Gamma \\ Y \end{bmatrix} \\ \begin{bmatrix} \Gamma \\ Y \end{bmatrix}^\top Q^\top [\hat{E}_A \hat{E}_B]^\top & -\Gamma + \epsilon_\Gamma I_n \end{bmatrix} \preceq 0 \quad (50a)$$

$$\forall (\hat{E}_A, \hat{E}_B) \in \mathcal{C} \text{ and } \forall Q \in \bar{\mathcal{Q}}, \quad (50b)$$

and let  $u = Kx$  with  $K = Y\Gamma^{-1}$ , then there exists a region of attraction  $\mathcal{B}_{r_0}$  with

$$r_0 = \min \left\{ r, \sqrt{\frac{\lambda_{\max}(\Gamma)\lambda_{\min}(\Gamma)}{\lambda_{\max}^2(\Gamma) - \epsilon_\Gamma \lambda_{\min}(\Gamma)}} \cdot r \right\}, \quad (51)$$

and the closed-loop system  $x^+ = (A(x) + B(x)K)x$  starting from any  $x(0) \in \mathcal{B}_{r_0}$  will exponentially converge to the origin.

*Proof.* Assumption 2 ensures that the actual system is in the set  $\mathcal{C}$ , i.e.,  $[\hat{E}_A \hat{E}_B] \in \mathcal{C}$ , thus (50) implies

$$\begin{aligned}
&\begin{bmatrix} -\Gamma & [\hat{E}_A \hat{E}_B] Q \begin{bmatrix} \Gamma \\ Y \end{bmatrix} \\ * & -\Gamma + \epsilon_\Gamma I_n \end{bmatrix} \preceq 0 \quad \forall Q \in \bar{\mathcal{Q}} \\
&\Updownarrow \\
&\begin{bmatrix} -\Gamma & [\hat{E}_A \hat{E}_B] \begin{bmatrix} Q_A \Gamma \\ Q_B Y \end{bmatrix} \\ * & -\Gamma + \epsilon_\Gamma I_n \end{bmatrix} \preceq 0 \quad \forall \text{blkdiag}(Q_A, Q_B) \in \text{conv}(\bar{\mathcal{Q}}) \\
&\Downarrow (49) \\
&\begin{bmatrix} -\Gamma & E_A \Xi_A(x) \Gamma + E_B \Xi_B(x) Y \\ * & -\Gamma + \epsilon_\Gamma I_n \end{bmatrix} \preceq 0 \quad \forall x \in \mathcal{B}_r \\
&\Downarrow (38) \\
&\begin{bmatrix} -\Gamma & A(x) \Gamma + B(x) Y \\ * & -\Gamma + \epsilon_\Gamma I_n \end{bmatrix} \preceq 0 \quad \forall x \in \mathcal{B}_r, \quad (52)
\end{aligned}$$

which corresponds to (12) in the proof of Theorem 1. Then following analogous arguments as in the proof of Theorem 1, we can complete the proof of this lemma.  $\square$

The set  $\mathcal{C}$  in (50b) is handled by Petersen's lemma [15], as detailed below.

**Lemma 5.** Under Assumption 3, if there exist  $\bar{\Gamma} \succ 0$ ,  $\epsilon_{\bar{\Gamma}} > 0$  and  $\bar{Y}$  such that

$$\begin{bmatrix} -\bar{\Gamma} - \mathbf{C} & 0 & \mathbf{B} \\ 0 & -\bar{\Gamma} + \epsilon_{\bar{\Gamma}} I_n & -\begin{bmatrix} \bar{\Gamma} \\ \bar{Y} \end{bmatrix}^T Q^T \\ \mathbf{B}^T & -Q \begin{bmatrix} \bar{\Gamma} \\ \bar{Y} \end{bmatrix} & -\mathbf{A} \end{bmatrix} \preceq 0 \quad \forall Q \in \bar{\mathcal{Q}}, \quad (53)$$

then (50) holds for some  $\Gamma \succ 0$ ,  $\epsilon_{\Gamma} > 0$  and  $Y$ . Conversely, suppose additionally  $\mathbf{B}\mathbf{A}^{-1}\mathbf{B}^T - \mathbf{C} \neq 0$ , then (50) implies (53).

*Proof.* By Assumption 3 and Schur complement, (53) is equivalent to

$$0 \succeq \begin{bmatrix} -\bar{\Gamma} - \mathbf{C} & 0 \\ * & -\bar{\Gamma} + \epsilon_{\bar{\Gamma}} I_n \end{bmatrix} + \begin{bmatrix} \mathbf{B} \\ -\begin{bmatrix} \bar{\Gamma} \\ \bar{Y} \end{bmatrix}^T Q^T \end{bmatrix} \cdot \mathbf{A}^{-1} \begin{bmatrix} * \end{bmatrix}^T$$

for all  $Q \in \bar{\mathcal{Q}}$ . Bearing in mind the definitions of  $\mathbf{Z}_c$  and  $\mathbf{Q}$  as in (44b), the above inequality equivalently rewrites as

$$0 \succeq \begin{bmatrix} -\bar{\Gamma} & \mathbf{Z}_c Q \begin{bmatrix} \bar{\Gamma} \\ \bar{Y} \end{bmatrix} \\ * & -\bar{\Gamma} + \epsilon_{\bar{\Gamma}} I_n \end{bmatrix} + \begin{bmatrix} \mathbf{Q} & 0 \\ 0 & 0 \end{bmatrix} + \begin{bmatrix} 0 & 0 \\ 0 & \begin{bmatrix} \bar{\Gamma} \\ \bar{Y} \end{bmatrix}^T Q^T \mathbf{A}^{-1} Q \begin{bmatrix} \bar{\Gamma} \\ \bar{Y} \end{bmatrix} \end{bmatrix}.$$

Multiplying both sides by  $\tau^{-1} > 0$  and letting

$$\Gamma = \tau^{-1} \bar{\Gamma}, \quad \epsilon_{\Gamma} = \tau^{-1} \epsilon_{\bar{\Gamma}}, \quad Y = \tau^{-1} \bar{Y}, \quad (54)$$

the above inequality is equivalent to

$$\begin{aligned} 0 \succeq & \begin{bmatrix} -\Gamma & \mathbf{Z}_c Q \begin{bmatrix} \Gamma \\ Y \end{bmatrix} \\ * & -\Gamma + \epsilon_{\Gamma} I_n \end{bmatrix} + \frac{1}{\tau} \begin{bmatrix} \mathbf{Q} & 0 \\ 0 & 0 \end{bmatrix} \\ & + \tau \begin{bmatrix} 0 & 0 \\ 0 & \begin{bmatrix} \Gamma \\ Y \end{bmatrix}^T Q^T \mathbf{A}^{-1} Q \begin{bmatrix} \Gamma \\ Y \end{bmatrix} \end{bmatrix}. \end{aligned} \quad (55)$$

By Petersen's Lemma reported in [15, Fact 2], the previous condition implies

$$\begin{aligned} 0 \succeq & \begin{bmatrix} -\Gamma & \mathbf{Z}_c Q \begin{bmatrix} \Gamma \\ Y \end{bmatrix} \\ * & -\Gamma + \epsilon_{\Gamma} I_n \end{bmatrix} + \begin{bmatrix} \mathbf{Q}^{1/2} \\ 0 \end{bmatrix} \Upsilon \begin{bmatrix} 0 & \mathbf{A}^{-1/2} Q \begin{bmatrix} \Gamma \\ Y \end{bmatrix} \end{bmatrix} \quad (56) \\ & + \begin{bmatrix} 0 \\ \begin{bmatrix} \Gamma \\ Y \end{bmatrix}^T Q^T \mathbf{A}^{-1/2} \end{bmatrix} \Upsilon^T \begin{bmatrix} \mathbf{Q}^{1/2} & 0 \end{bmatrix} \quad \forall \Upsilon \text{ with } \Upsilon \Upsilon^T \preceq I_n. \end{aligned}$$

Note that (56) is a necessary and sufficient condition for (55) under the additional condition  $\mathbf{Q} \neq 0$ , i.e.,  $\mathbf{B}\mathbf{A}^{-1}\mathbf{B}^T - \mathbf{C} \neq 0$  [15, Fact 2]. According to (44), (56) is equivalent to

$$\begin{bmatrix} -\Gamma & ZQ \begin{bmatrix} \Gamma \\ Y \end{bmatrix} \\ * & -\Gamma + \epsilon_{\Gamma} I_n \end{bmatrix} \preceq 0 \quad \forall Z \in \mathcal{C},$$

which corresponds to (50). This completes the proof.  $\square$

The next result, obtained from Lemma 4 and Lemma 5, is the solution to Problem 2.

**Theorem 4.** Under Assumptions 1, 2 and 3, given a positive real number  $r$  and the set  $\mathcal{B}_r$ , if there exist  $\bar{\Gamma} \succ 0$ ,  $\epsilon_{\bar{\Gamma}} > 0$  and  $\bar{Y}$  such that (53) holds, and let  $u = Kx$  with  $K = \bar{Y}\bar{\Gamma}^{-1}$ , then there exists a region of attraction  $\mathcal{B}_{\bar{r}_0}$  with

$$\bar{r}_0 = \min \left\{ r, \sqrt{\frac{\lambda_{\max}(\bar{\Gamma})\lambda_{\min}(\bar{\Gamma})}{\lambda_{\max}^2(\bar{\Gamma}) - \epsilon_{\bar{\Gamma}}\lambda_{\min}(\bar{\Gamma})}} \cdot r \right\}, \quad (57)$$

and the closed-loop system  $x^+ = (A(x) + B(x)K)x$  starting from any  $x(0) \in \mathcal{B}_{\bar{r}_0}$  will exponentially converge to the origin.

*Proof.* Under Assumption 3 and by Lemma 5, (53) implies (50), which, under Assumptions 1 and 2, leads to the result of this theorem by Lemma 4. In addition, (51) converts to (57) by (54).  $\square$

**Example 4.** Consider the system (13) as in Example 1. In this case, we know vector-valued continuous functions

$$\begin{aligned} \xi_{A_1}(x) &= \left(1, \frac{\sin x_1}{x_1}\right), \quad \xi_{A_2}(x) = (1, x_1, x_1^2), \\ \xi_{B_1}(x) &= (1, |x_1|, |x_2|, e^{x_1}, e^{x_2}). \end{aligned}$$

Assumption 1 allows us to write the state-dependent representation as  $A(x) = E_A \text{blkdiag}(\xi_{A_1}(x), \xi_{A_2}(x))$  and  $B(x) = E_B \xi_{B_1}(x)$  with

$$E_A = \begin{bmatrix} 1 & 0.1 & 0.2 & 0 & 0 \\ 0.2 & 0 & 0.9 & 0 & 0.1 \end{bmatrix}, \quad E_B = \begin{bmatrix} 0.1 & 0 & 0.1 & 0 & 0 \\ 0 & 0 & 0 & 0.1 & 0 \end{bmatrix}.$$

Note that the system knowledge  $E_A$  and  $E_B$  are unknown in the controller design. As in (39), apply experimental input  $u_d$ , uniformly distributed within the interval  $[-1.3, 1.3]$ , to collect data: 10 experiments are performed each consisting of 13 data samples. The experimental noise  $d$  is randomly selected within the energy bound  $\Theta = 0.0021I_2$  as in Assumption 2. We store the data samples into  $X_0 \in \mathbb{R}^{5 \times 130}$ ,  $X_1 \in \mathbb{R}^{2 \times 130}$ ,  $U_0 \in \mathbb{R}^{5 \times 130}$  as in (40). Take  $r = 0.92$  for  $\mathcal{B}_r$ . By (47), we have the set  $\bar{\mathcal{Q}}$  as in (48). Solving (53) in Theorem 4 via CVX yields  $\epsilon_{\bar{\Gamma}} = 0.000045$ ,  $\bar{Y} = [-0.0178 \ -0.0186]$ ,  $\bar{\Gamma} = \begin{bmatrix} 0.0082 & 0.0000 \\ 0.0000 & 0.0082 \end{bmatrix}$ , and  $K = [-2.1797 \ -2.2750]$ . According to (57), the estimate of ROA,  $\mathcal{B}_{\bar{r}_0}$ , has a radius of  $\bar{r}_0 = 0.92$ . Figure 4 is the phase portrait of the closed-loop system  $x^+ = A(x)x + B(x)Kx$ .  $\square$

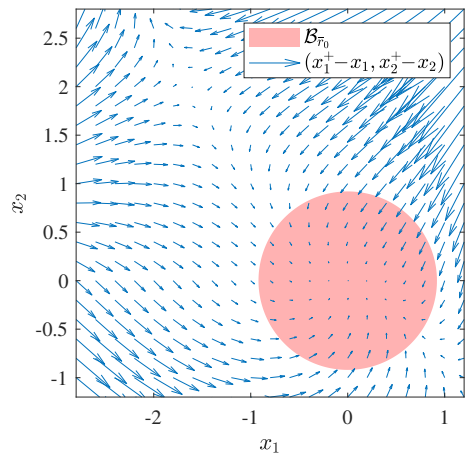


Fig. 4. Phase portrait of the closed-loop system with data-driven controller.

### C. Robustness Against Disturbances

As discussed in Section II-C and Theorem 2, the model-based controller is robust against disturbances. The same result applies to the data-driven controller, which is detailed in the next theorem.

**Theorem 5.** Under Assumptions 1, 2 and 3, given a positive real number  $r$  and the set  $\mathcal{B}_r$ , suppose that there exist  $\bar{\Gamma} \succ 0$ ,  $\epsilon_{\bar{\Gamma}} > 0$  and  $\bar{Y}$  such that (53) holds, and let  $K = \bar{Y}\bar{\Gamma}^{-1}$  for the disturbed closed-loop system

$$x^+ = (A(x) + B(x)K)x + w.$$

If the initial state  $x(0)$  and disturbance  $w(k)$  satisfy

$$|x(0)|^2 \leq r^2 \text{ and } \bar{\delta}_{x_0}|x(0)|^2 + \bar{\delta}_w|w|_\infty^2 \leq r^2, \quad (58a)$$

where

$$\bar{\delta}_{x_0} := \frac{2\lambda_{\max}^2(\bar{\Gamma}) - \epsilon_{\bar{\Gamma}}\lambda_{\min}(\bar{\Gamma})}{2\lambda_{\min}(\bar{\Gamma})\lambda_{\max}(\bar{\Gamma})}, \quad (58b)$$

$$\bar{\delta}_w := \frac{4\gamma_{A_{\text{cl}}}^2\lambda_{\max}^5(\bar{\Gamma}) + 2\epsilon_{\bar{\Gamma}}\lambda_{\min}(\bar{\Gamma})\lambda_{\max}^3(\bar{\Gamma})}{\epsilon_{\bar{\Gamma}}^2\lambda_{\min}^3(\bar{\Gamma})}, \quad (58c)$$

$$\gamma_{A_{\text{cl}}} := \max_{x \in \mathcal{B}_r} \|A(x) + B(x)K\|, \quad (58d)$$

then there exists  $\bar{\beta} \in \mathcal{KL}$  and  $\bar{\gamma} \in \mathcal{K}$  such that

$$|x(k)| \leq \bar{\beta}(x(0), k) + \bar{\gamma}(|w|_\infty) \quad \forall k \in \mathbb{N}. \quad (59)$$

*Proof.* Under Assumption 3 and by Lemma 5, (53) implies (50). Under Assumptions 1, 2 and by Lemma 4, (50) implies (52), which corresponds to (12). Following the proof of Theorem 1, (52) [or (12)] leads to (17). Using analogous arguments as in the proof of Theorem 2, we can prove this Theorem 5. In addition, (15) converts to (58) by (54).  $\square$

**Remark 1.** The parameter values in (15),  $\delta_{x_0}$ ,  $\delta_w$  and  $\gamma_{A_{\text{cl}}}$ , are all accessible and computable in the model-based case. However, in the data-driven case, the value of  $\gamma_{A_{\text{cl}}}$  as defined in (58d) is unavailable due to the lack of model knowledge. Instead, a computable upper bound of  $\gamma_{A_{\text{cl}}}$  can be derived and used in its place, that is,

$$\begin{aligned} \gamma_{A_{\text{cl}}} &:= \max_{x \in \mathcal{B}_r} \|A(x) + B(x)K\| \\ &\stackrel{(38)}{=} \max_{x \in \mathcal{B}_r} \left\| [E_A \ E_B] \begin{bmatrix} \Xi_A(x)x \\ \Xi_B(x)Kx \end{bmatrix} \right\| \\ &\leq \| [E_A \ E_B] \| \max_{x \in \mathcal{B}_r} \left\| \begin{bmatrix} \Xi_A(x)x \\ \Xi_B(x)Kx \end{bmatrix} \right\| \\ &\stackrel{(44)}{\leq} \left( \|\mathbf{Z}_c\| + \|\mathbf{Q}^{\frac{1}{2}}\| \|\mathbf{A}^{-\frac{1}{2}}\| \right) \max_{x \in \mathcal{B}_r} \left\| \begin{bmatrix} \Xi_A(x)x \\ \Xi_B(x)Kx \end{bmatrix} \right\| \\ &=: \bar{\gamma}_{A_{\text{cl}}}. \end{aligned}$$

The upper bound  $\bar{\gamma}_{A_{\text{cl}}}$ , which is computable from data alone, can be used to replace  $\gamma_{A_{\text{cl}}}$  in (58d).  $\blacksquare$

**Example 5.** Following Example 4, the controller  $K$  remains unchanged. For the closed-loop system  $x^+ = A(x)x + B(x)Kx + w$ , we set  $x(0) = (-0.4, -0.4)$  and the disturbance  $(w_1, w_2)$  as random variables uniformly distributed in the interval  $[-0.1, 0.1]$ . The simulation result is depicted in Figure 5, which is consistent with (59) in Theorem 5.  $\triangleleft$

#### D. System Subject to Input Saturation

This subsection presents a data-driven controller for the system with input saturation, along with an estimate of ROA.

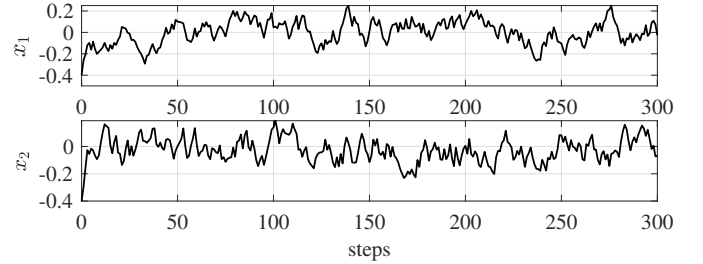


Fig. 5. State response of the closed-loop system with data-driven controller under disturbance.

**Theorem 6.** Under Assumptions 1, 2 and 3, given a positive real number  $r$  and the set  $\mathcal{B}_r$ , if there exist  $\bar{\Gamma} \succ 0$ ,  $\epsilon_{\bar{\Gamma}} > 0$ ,  $\bar{Y}$ ,  $\bar{W}$  and diagonal positive definite matrix  $\bar{S}$  such that

$$\begin{bmatrix} \bar{\Gamma} & \bar{W}_{(i)}^\top \\ \bar{W}_{(i)} & \bar{u}_i^2 \end{bmatrix} \succeq 0 \quad i = 1, \dots, m, \quad (60a)$$

$$\begin{bmatrix} -\bar{\Gamma} + \epsilon_{\bar{\Gamma}}I_n & -\bar{Y}^\top - \bar{W}^\top & 0 & \begin{bmatrix} \bar{\Gamma} \\ \bar{Y} \end{bmatrix}^\top Q^\top \\ -\bar{Y} - \bar{W} & -2\bar{S} & 0 & \begin{bmatrix} 0 \\ \bar{S} \end{bmatrix}^\top Q^\top \\ 0 & 0 & -\bar{\Gamma} - \mathbf{C} & -\mathbf{B} \\ Q \begin{bmatrix} \bar{\Gamma} \\ \bar{Y} \end{bmatrix} & Q \begin{bmatrix} 0 \\ \bar{S} \end{bmatrix} & -\mathbf{B}^\top & -\mathbf{A} \end{bmatrix} \succeq 0 \quad \forall Q \in \bar{\mathcal{Q}} \quad (60b)$$

and let  $u = Kx$  with  $K = \bar{Y}\bar{\Gamma}^{-1}$ , then there exists a region of attraction  $\mathcal{B}_{\bar{r}_0} \cap \mathcal{E}_{\bar{P},1}$  with  $\bar{P} = \bar{\Gamma}^{-1}$  and

$$\bar{r}_0 = \min \left\{ r, \sqrt{\frac{\lambda_{\max}(\bar{\Gamma})\lambda_{\min}(\bar{\Gamma})}{\lambda_{\max}^2(\bar{\Gamma}) - \epsilon_{\bar{\Gamma}}\lambda_{\min}(\bar{\Gamma})}} \cdot r \right\}, \quad (61)$$

and the closed-loop system  $x^+ = A(x)x + B(x)\text{sat}(Kx)$  starting from any  $x(0) \in \mathcal{B}_{\bar{r}_0} \cap \mathcal{E}_{\bar{P},1}$  will exponentially converge to the origin.

*Proof.* Following analogous arguments as in the proof of Theorem 3, inequalities (60a) imply  $\mathcal{E}_{\bar{P},1} \subseteq \mathcal{S}(L)$  with  $L = \bar{W}\bar{\Gamma}^{-1}$ . By Lemma 2, we conclude that (60a) results in

$$\phi(u)^\top N(\text{sat}(u) + Lx) \leq 0 \quad \forall x \in \mathcal{E}_{\bar{P},1} \quad (62)$$

for any diagonal positive definite matrix  $N$ .

By Schur complement and the definitions of  $\mathbf{Z}_c$  and  $\mathbf{Q}$  in (44b), the linear matrix inequality in (60b) is equivalent to

$$\begin{aligned} 0 &\succeq \begin{bmatrix} -\bar{\Gamma} + \epsilon_{\bar{\Gamma}}I_n & * & * \\ -\bar{Y} - \bar{W} & -2\bar{S} & * \\ \mathbf{Z}_c Q \begin{bmatrix} \bar{\Gamma} \\ \bar{Y} \end{bmatrix} & \mathbf{Z}_c Q \begin{bmatrix} 0 \\ \bar{S} \end{bmatrix} & -\bar{\Gamma} \end{bmatrix} + \begin{bmatrix} 0 & * & * \\ 0 & 0 & * \\ 0 & 0 & \mathbf{Q} \end{bmatrix} \\ &+ \begin{bmatrix} \begin{bmatrix} \bar{\Gamma} \\ \bar{Y} \end{bmatrix}^\top Q^\top \mathbf{A}^{-1} Q \begin{bmatrix} \bar{\Gamma} \\ \bar{Y} \end{bmatrix} & * & * \\ \begin{bmatrix} 0 \\ \bar{S} \end{bmatrix}^\top Q^\top \mathbf{A}^{-1} Q \begin{bmatrix} \bar{\Gamma} \\ \bar{Y} \end{bmatrix} & \begin{bmatrix} 0 \\ \bar{S} \end{bmatrix}^\top Q^\top \mathbf{A}^{-1} Q \begin{bmatrix} 0 \\ \bar{S} \end{bmatrix} & * \\ 0 & 0 & 0 \end{bmatrix}. \end{aligned}$$

Multiplying both sides by  $\tau^{-1} > 0$  and letting

$$\begin{aligned} \Gamma &= \tau^{-1}\bar{\Gamma}, \quad \epsilon_\Gamma = \tau^{-1}\epsilon_{\bar{\Gamma}}, \quad Y = \tau^{-1}\bar{Y}, \\ W &= \tau^{-1}\bar{W}, \quad S = \tau^{-1}\bar{S}, \end{aligned} \quad (63)$$

the above matrix inequality is equivalent to

$$0 \succeq \begin{bmatrix} -\Gamma + \epsilon_\Gamma I_n & * & * \\ -Y - W & -2S & * \\ \mathbf{Z}_c Q \begin{bmatrix} \Gamma \\ Y \end{bmatrix} & \mathbf{Z}_c Q \begin{bmatrix} 0 \\ S \end{bmatrix} & -\Gamma \end{bmatrix} + \frac{1}{\tau} \begin{bmatrix} 0 & * & * \\ 0 & 0 & * \\ 0 & 0 & \mathbf{Q} \end{bmatrix} \\ + \tau \begin{bmatrix} \begin{bmatrix} \Gamma \\ Y \end{bmatrix}^\top Q^\top \mathbf{A}^{-1} Q \begin{bmatrix} \Gamma \\ Y \end{bmatrix} & * & * \\ \begin{bmatrix} 0 \\ S \end{bmatrix}^\top Q^\top \mathbf{A}^{-1} Q \begin{bmatrix} \Gamma \\ Y \end{bmatrix} & \begin{bmatrix} 0 \\ S \end{bmatrix}^\top Q^\top \mathbf{A}^{-1} Q \begin{bmatrix} 0 \\ S \end{bmatrix} & * \\ 0 & 0 & 0 \end{bmatrix}.$$

By Petersen's Lemma reported in [15, Fact 2], the previous inequality implies

$$0 \succeq \begin{bmatrix} -\Gamma + \epsilon_\Gamma I_n & * & * \\ -Y - W & -2S & * \\ \mathbf{Z}_c Q \begin{bmatrix} \Gamma \\ Y \end{bmatrix} & \mathbf{Z}_c Q \begin{bmatrix} 0 \\ S \end{bmatrix} & -\Gamma \end{bmatrix} \\ + \begin{bmatrix} 0 & * & * \\ 0 & 0 & * \\ \mathbf{Q}^{1/2} \Upsilon \mathbf{A}^{-1/2} Q \begin{bmatrix} \Gamma \\ Y \end{bmatrix} & \mathbf{Q}^{1/2} \Upsilon \mathbf{A}^{-1/2} Q \begin{bmatrix} 0 \\ S \end{bmatrix} & 0 \end{bmatrix}$$

for all  $\Upsilon$  with  $\Upsilon \Upsilon^\top \preceq I_n$ . Under Assumption 3 and (44), the above condition is equivalent to

$$\begin{bmatrix} -\Gamma + \epsilon_\Gamma I_n & * & * \\ -Y - W & -2S & * \\ ZQ \begin{bmatrix} \Gamma \\ Y \end{bmatrix} & ZQ \begin{bmatrix} 0 \\ S \end{bmatrix} & -\Gamma \end{bmatrix} \preceq 0 \quad \forall Z \in \mathcal{C}.$$

Note that Assumption 2 ensures that  $[E_A \ E_B] \in \mathcal{C}$ . So far, by the above conditions, we have established that (60b) implies that

$$\begin{bmatrix} -\Gamma + \epsilon_\Gamma I_n & * & * \\ -Y - W & -2S & * \\ E_A Q_A \Gamma + E_B Q_B Y & E_B Q_B S & -\Gamma \end{bmatrix} \preceq 0$$

for all  $\text{blkdiag}(Q_A, Q_B) \in \bar{\mathcal{Q}}$ , which further implies, by (49) and (38), that

$$\begin{bmatrix} -\Gamma + \epsilon_\Gamma I_n & * & * \\ -Y - W & -2S & * \\ A(x)\Gamma + B(x)Y & B(x)S & -\Gamma \end{bmatrix} \preceq 0 \quad \forall x \in \mathcal{B}_r.$$

Let

$$\begin{aligned} N &= S^{-1}, & Y &= K\Gamma, & W &= L\Gamma, \\ P &= \Gamma^{-1}, & \epsilon &= \epsilon_\Gamma / \lambda_{\max}^2(\Gamma). \end{aligned} \tag{64}$$

Pre- and post-multiplying both sides of the above inequality by  $\text{blkdiag}(P, N, I_n)$  results in

$$\begin{bmatrix} -P + \epsilon I_n & * & * \\ -N(K + L) & -2N & * \\ A(x) + B(x)K & B(x) & -P^{-1} \end{bmatrix} \preceq 0 \quad \forall x \in \mathcal{B}_r.$$

By Schur complement, the above inequality is equivalent to  $H(x) \preceq 0$  for all  $x \in \mathcal{B}_r$ , where  $H(x)$  has the same expression as in (35). This fact implies, for  $V(x) := x^\top P x$ , that

$$\begin{aligned} & \begin{bmatrix} x \\ \phi(Kx) \end{bmatrix}^\top H(x) \begin{bmatrix} x \\ \phi(Kx) \end{bmatrix} \leq 0 \quad \forall x \in \mathcal{B}_r \\ \xleftarrow{(25),(28)} \quad & V(x^+) - V(x) \\ & -2\phi(Kx)^\top N(\text{sat}(Kx) + Lx) \leq -\epsilon|x|^2 \quad \forall x \in \mathcal{B}_r. \end{aligned}$$

Because of (60a) and (62), we obtain

$$V(x^+) - V(x) \leq -\epsilon|x|^2 \quad \forall x \in \mathcal{B}_r \cap \mathcal{E}_{\bar{P},1}$$

$$\hat{\mathbb{P}} P = \tau \bar{P} \text{ and } \mathcal{E}_{\bar{P},1} = \mathcal{E}_{P,\tau}$$

$$V(x^+) - V(x) \leq -\epsilon|x|^2 \quad \forall x \in \mathcal{B}_r \cap \mathcal{E}_{P,\tau},$$

which is consistent with (29). Then by Lemma 3, and rewriting (30) to (61) via  $\epsilon = \epsilon_\Gamma / \lambda_{\max}^2(\Gamma)$ ,  $\lambda_{\max}(P) = \lambda_{\min}^{-1}(\Gamma)$ ,  $\lambda_{\min}(P) = \lambda_{\max}^{-1}(\Gamma)$ , and (63), we complete the proof.  $\square$

**Example 6.** Following Example 4, the experimental data  $X_0$ ,  $X_1$ ,  $U_0$  and the energy bound  $\Theta$  remain unchanged. Take  $r = 0.92$  for  $\mathcal{B}_r$ . By (7), we have the set  $\bar{\mathcal{Q}}$  as in (48). For different level of the saturation  $\bar{u} \in \{2.0, 1.0, 0.5, 0.25\}$ , solving (60) in Theorem 6 via CVX yields  $K = [-2.5369 - 2.9559]$ ,  $[-2.5369 - 2.9559]$ ,  $[-2.5369 - 2.9559]$  and  $[-2.6885 - 2.2310]$ , respectively. Note that the program (60) in Theorem 6 is only a feasibility problem, hence we set minimizing  $[\lambda_{\max}(\bar{\Gamma}) - \lambda_{\min}(\bar{\Gamma}) - 2\text{trace}(\bar{\Gamma})]$  as the objective when solving the LMIs (60). The estimate of ROA,  $\mathcal{B}_{\bar{r}_0} \cap \mathcal{E}_{\bar{P},1}$ , for different values of  $\bar{u}$  is shown in Figure 6.  $\triangleleft$

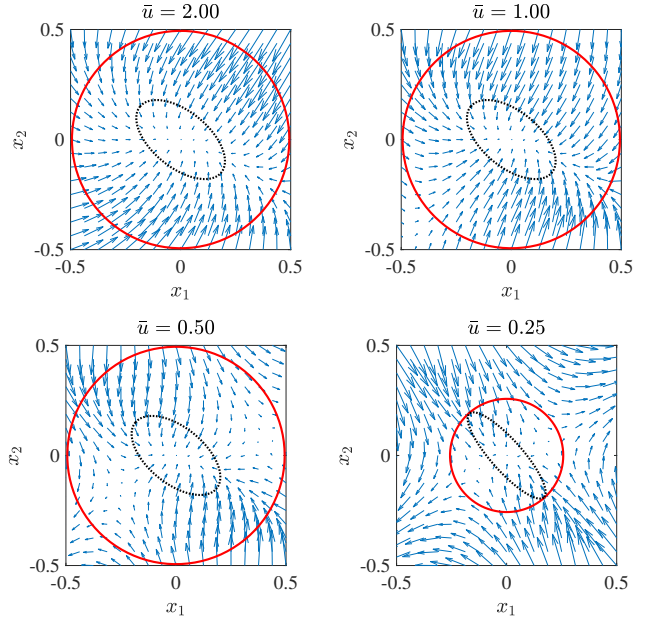


Fig. 6. Estimate of ROA,  $\mathcal{B}_{\bar{r}_0} \cap \mathcal{E}_{\bar{P},1}$ , for different saturation levels. The red solid ball is  $\mathcal{B}_{\bar{r}_0}$ ; the black dashed ellipsoid is  $\mathcal{E}_{\bar{P},1}$ ; the background is the phase portrait regarding the closed-loop system  $x^+ = A(x)x + B(x)\text{sat}(Kx)$ .

### E. Discussion on Region of Attraction

While the ROA is directly estimated as  $\mathcal{B}_{\bar{r}_0}$  in Theorem 1, this is not the only method. In the model-based case, the closed-loop system  $x^+ = A(x)x + B(x)Kx$  is known, and the Lyapunov function is given by  $V(x) = x^\top \Gamma^{-1}x$ , where  $\Gamma$  is computed from (10). Then  $V(x^+) - V(x) = v(x)$  with

$$v(x) := [*]^\top \Gamma^{-1} \cdot [A(x)x + B(x)Kx] - x^\top \Gamma^{-1}x,$$

and we can numerically determine the set

$$\mathcal{V} := \{x : v(x) < 0\}.$$

Any sublevel set  $\mathcal{E}_{\Gamma^{-1}, \gamma} := \{x \in \mathbb{R}^n : x^\top \Gamma^{-1}x \leq \gamma\}$  contained in  $\mathcal{V} \cup \{0\}$  is an estimate of ROA for the closed-loop system. Moreover, the union of the set  $\mathcal{B}_{\bar{r}_0}$  and the largest

sublevel set  $\mathcal{E}_{\Gamma^{-1},\gamma}$  contained in  $\mathcal{V} \cup \{0\}$ , i.e.,  $\mathcal{B}_{r_0} \cup \mathcal{E}_{\Gamma^{-1},\gamma}$ , is also an ROA.

When the system is subject to input saturation, the same procedure applies. The closed-loop system is  $x^+ = A(x)x + B(x)\text{sat}(Kx)$ , and the Lyapunov function is given by  $V(x) = x^\top \Gamma^{-1}x$ , where  $\Gamma$  is computed from (32). Then,  $V(x^+) - V(x) = v_{\text{sat}}(x)$  with

$$v_{\text{sat}}(x) := [*]^\top \Gamma^{-1} \cdot [A(x)x + B(x)\text{sat}(Kx)] - x^\top \Gamma^{-1}x,$$

and we can *numerically* determine the set

$$\mathcal{V}_{\text{sat}} := \{x : v_{\text{sat}}(x) < 0\}.$$

Any sublevel set  $\mathcal{E}_{\Gamma^{-1},\gamma}$  contained in  $\mathcal{V}_{\text{sat}} \cup \{0\}$  is an estimate of ROA for the closed-loop system. The union of the set  $\mathcal{B}_{r_0} \cap \mathcal{E}_{\Gamma^{-1},1}$ , estimated by Theorem 3, and the largest sublevel set  $\mathcal{E}_{\Gamma^{-1},\gamma}$  contained in  $\mathcal{V}_{\text{sat}} \cup \{0\}$ , i.e.,  $\{\mathcal{B}_{r_0} \cap \mathcal{E}_{\Gamma^{-1},1}\} \cup \mathcal{E}_{\Gamma^{-1},\gamma}$ , is also an ROA.

In the data-driven case, although  $v(x)$  is not accessible and the set  $\mathcal{V}$  cannot be characterized due to the lack of model knowledge, we can still upper bound  $v(x)$  with a quantity that is computable from data alone. By Assumption 1 and (38), the closed-loop system is  $x^+ = E_A \Xi_A(x)x + E_B \Xi_B(x)Kx$ . Assumption 2 ensures  $[E_A \ E_B] \in \mathcal{C}$ . Assumption 3 allows us to express the set  $\mathcal{C}$  in the form of (44), which means

$$[E_A \ E_B] = \mathbf{Z}_c + \mathbf{Q}^{1/2} \Upsilon \mathbf{A}^{-1/2} \text{ for a } \Upsilon \text{ with } \|\Upsilon\| \leq 1,$$

where  $\mathbf{Z}_c$ ,  $\mathbf{Q}$  and  $\mathbf{A}$  are defined by data. The Lyapunov function is given by  $V(x) = x^\top \Gamma^{-1}x$ . Bearing in mind that  $\Gamma^{-1} = \tau \bar{\Gamma}^{-1}$ ,  $\tau > 0$  as in (54), and  $\bar{\Gamma}$  calculated from (53), we have

$$\begin{aligned} & V(x^+) - V(x) \\ &= [*]^\top \Gamma^{-1} \cdot [E_A \ E_B] \begin{bmatrix} \Xi_A(x)x \\ \Xi_B(x)Kx \end{bmatrix} - x^\top \Gamma^{-1}x \\ &\leq \tau \underbrace{\left( -x^\top \bar{\Gamma}^{-1}x + v_1(x) + v_2(x) + v_3(x) \right)}_{=: v_{\text{data}}(x)} \end{aligned}$$

where

$$\begin{aligned} v_1(x) &:= \begin{bmatrix} \Xi_A(x)x \\ \Xi_B(x)Kx \end{bmatrix}^\top \mathbf{Z}_c^\top \bar{\Gamma}^{-1} \mathbf{Z}_c \begin{bmatrix} \Xi_A(x)x \\ \Xi_B(x)Kx \end{bmatrix}, \\ v_2(x) &:= 2 \left| \mathbf{Q}^{\frac{1}{2}} \bar{\Gamma}^{-1} \mathbf{Z}_c \begin{bmatrix} \Xi_A(x)x \\ \Xi_B(x)Kx \end{bmatrix} \right| \left| \mathbf{A}^{-\frac{1}{2}} \begin{bmatrix} \Xi_A(x)x \\ \Xi_B(x)Kx \end{bmatrix} \right|, \\ v_3(x) &:= \left| \mathbf{Q}^{\frac{1}{2}} \bar{\Gamma}^{-1} \mathbf{Q}^{\frac{1}{2}} \right| \left| \mathbf{A}^{-\frac{1}{2}} \begin{bmatrix} \Xi_A(x)x \\ \Xi_B(x)Kx \end{bmatrix} \right|^2, \end{aligned}$$

which are all computable from data alone. Next, we can *numerically* determine the set

$$\mathcal{V}_{\text{data}} := \{x : v_{\text{data}}(x) < 0\}.$$

Any sublevel set  $\mathcal{E}_{\bar{\Gamma}^{-1},\gamma}$  contained in  $\mathcal{V}_{\text{data}} \cup \{0\}$  is an estimate of ROA for the closed-loop system. Moreover, the union of the set  $\mathcal{B}_{\bar{r}_0}$  and the largest sublevel set  $\mathcal{E}_{\bar{\Gamma}^{-1},\gamma}$  contained in  $\mathcal{V}_{\text{data}} \cup \{0\}$ , i.e.,  $\mathcal{B}_{\bar{r}_0} \cup \mathcal{E}_{\bar{\Gamma}^{-1},\gamma}$ , is also an ROA.

When the system is subject to input saturation, the same procedure applies in the data-driven case, and we omit the details due to space limitations.

#### IV. COMPARISONS WITH EXISTING METHODS

We compare our proposed method with existing methods in this section.

*State-Dependent Riccati Equation:* As summarized in the survey [40], a model-based controller for (1) in continuous-time case is in the form  $u(x) = -R(x)^{-1}B(x)^\top P(x)x$ , where  $P(x)$  is the positive definite solution to the algebraic state-dependent Riccati equation (SDRE):  $P(x)A(x) + A(x)^\top P(x) - P(x)B(x)R(x)^{-1}B(x)^\top P(x) + H(x) = 0$ , and  $R(x) \succ 0$ ,  $H(x) \succeq 0$  are design parameters. On the one hand, it is difficult to achieve or prove global asymptotic stability unless the closed-loop model possesses a special structure [40, §4.2]. On the other hand, an analytical solution to the SDRE cannot be obtained in general, and a practical approach is to solve the SDRE online at a relatively high rate [40, §7.1]. In the data-driven context, [35] solves the SDRE at each control instant via data-dependent LMIs. Solving LMIs online incurs substantial computational cost, and the user has to balance computation time and control frequency. The recursive feasibility of LMIs is another critical issue, which is partially addressed in [36] in the case of noise-free data. In contrast, our approach is applicable to noisy data and computes the controller offline. The resulting controller is then implemented with a certified estimate of ROA under input saturation, along with guaranteed robustness against disturbances.

*Sum-of-Squares:* In polynomial control systems, sum-of-squares (SOS) programming has been extensively used [45]. By employing SOS, [14]–[17] design data-driven controllers that guarantee global asymptotic stability for polynomial systems. For more general classes of nonlinear systems, their dynamics can be approximated by polynomials [18]–[20], enabling the synthesis of data-driven controllers via SOS. However, such polynomial approximations are typically local [24, §4.1], and accounting for approximation errors and data noise introduces conservatism. Leveraging the Koopman operator, [27] derives a data-based finite-dimensional bilinear surrogate model with truncation error. Following [27], [46] formulates an SOS program for controller design. In general, the truncation (or approximation) error is difficult to characterize, since it depends on the system dynamics, the selected lifted coordinates, and the data samples. Under suitable assumptions, [27] gives bounds on the approximation error. As previously noted, the approximation error, along with data noise, inevitably introduces additional conservatism. In contrast, our proposed approach differs from the aforementioned literature in three aspects. First, our data-based system representation builds on a function library (cf. Assumption 1), which is common for various systems such as electrical and mechanical ones. Assumption 1 allows us to avoid analyze the approximation errors if the data is rich enough and free of noise. Nevertheless, we recognize that our method also exhibits some conservatism, which mainly arises from the convex polytope, namely (9) and (49). Second, SOS programming inherently faces challenges in scalability, computational complexity, and numerical stability, especially when compared to the LMIs employed in our method. Third, our approach can analyze the robustness of the closed-loop system against disturbances and

incorporate the input saturation, which are not considered in the aforementioned works.

*Feedback Linearization and Nonlinearity Cancellation:* Via a suitable coordinate transformation, classes of systems can be feedback linearized, meaning that all nonlinearities are canceled by a feedback controller [37], [47]. To this end, the critical step is to find an appropriate coordinate transformation. In [28] and [29], the authors assume prior knowledge of the state transformation coordinates to design data-driven feedback linearizable controllers. [30] relaxes this assumption and learns the transformation directly from data. However, not all systems can be feedback linearized, as exemplified in (13). In such cases, [31] and [33] propose approaches to approximately cancel the nonlinearities and minimize their effects to achieve better performance. Here, we compare Theorem 4 with the methods in [31] numerically.

**Example 7.** In this numerical comparison, we use the same dataset as in Example 4 when applying the methods from [31]. As the dynamics of (13) are more general than [31, Eq. (1)], we resort to [31, Corollary 1]. However, this result assumes noise-free data, so we adapt [31, Lemma 3] to make [31, Corollary 1] applicable to noisy settings. For [31, Eq. (34)], we set  $\mathcal{Z}(x, u) = (x, u, \sin x_1 - x_1, x_1^2 x_2, |x_2|u, e^{x_1}u - u)$ . Take  $\Omega = I_3$  in [31, Eq. (48)]. Solving the data-based LMIs in [31] yields the controller  $u^+ = -2.5135x_1 - 1.4326x_2 + 0.2220u$ . The resulting Lyapunov function is  $V(\chi) = \chi^\top P_1^{-1}\chi$  with  $\chi := (x, u)$  and  $P_1^{-1} = \begin{bmatrix} 0.0261 & 0.0040 & 0.0048 \\ 0.0040 & 0.0154 & 0.0026 \\ 0.0048 & 0.0026 & 0.0020 \end{bmatrix}$ . The ROA is estimated using the adapted version of [31, Proposition 2], and is depicted in Figure 7. Specifically, the gray area in Figure 7 represents the set  $\mathcal{L}$  from [31, Proposition 2], where  $V(\chi^+) - V(\chi)$  is negative. The black dotted ellipsoid is the Lyapunov sublevel set  $\mathcal{R}_\gamma := \{\chi : V(\chi) \leq \gamma\}$  contained in  $\mathcal{L} \cup \{0\}$ , hence, it provides an estimate of ROA. Both sets  $\mathcal{L}$  and  $\mathcal{R}_\gamma$  are projected onto the plane  $\{\chi : \chi_3 = 0\}$ . The red solid circle in Figure 7 represents the ROA estimated by Theorem 4, which is larger than that obtained from [31]. We note that the calculation of  $\mathcal{L}$  in [31, Proposition 2] is based on an upper bound of  $V(\chi^+) - V(\chi)$ , which introduces additional conservatism. This may explain why our approach yields a larger estimate of ROA.  $\triangleleft$

## V. EXPERIMENT

### A. Numerical Experiment

This simulation is conducted to verify Theorem 4, the result on data-driven controller design. Consider the quadrotor aerial vehicle with attitude dynamics described by

$$\begin{cases} \dot{\eta} = T(\phi, \theta)\omega \\ J\dot{\omega} + \omega \times (J\omega) = M \end{cases}$$

where  $J = \text{blkdiag}(J_{11}, J_{22}, J_{33}) \in \mathbb{R}^{3 \times 3}$  is the inertia matrix with respect to the body-fixed frame;  $\omega \in \mathbb{R}^3$  is the angular velocity in the body-fixed frame;  $M \in \mathbb{R}^3$  is the total moment vector in the body-fixed frame;  $\times$  is the vector cross product;  $\eta = (\phi, \theta, \psi) \in \mathbb{R}^3$  is the vector of Euler angles (roll, pitch, yaw) that describe the attitude of

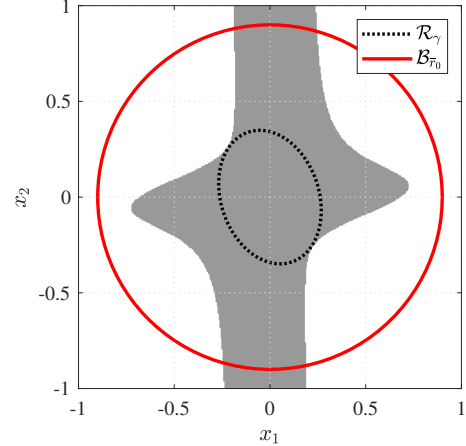


Fig. 7. Comparison results. The black dotted ellipsoid  $\mathcal{R}_\gamma$  is the ROA estimated by [31]; The red solid circle  $\mathcal{B}_{\bar{r}_0}$  is the ROA estimated by Theorem 4.

the quadrotor with respect to the inertial frame; the transformation matrix  $T(\phi, \theta)$  is given by [48, Eq. (5.67)]. Take  $J = \text{blkdiag}(0.01668, 0.01772, 0.02966)$ . Note that these parameter values are used solely for experimental data generation, not for the data-driven controller synthesis.

We discretize the continuous-time system using the forward Euler method with a sampling time  $h = 0.002$ . The resulting discrete-time system can be written in the form of (1), where  $x = (\eta, \omega)$ , and

$$A(x) = \begin{bmatrix} 1 & 0 & 0 & h & h \sin x_1 \tan x_2 & h \cos x_1 \tan x_2 \\ 0 & 1 & 0 & 0 & h \cos x_1 & -h \sin x_1 \\ 0 & 0 & 1 & 0 & h \frac{\sin x_1}{\cos x_2} & h \frac{\cos x_1}{\cos x_2} \\ 0 & 0 & 0 & 1 & 0 & h \frac{J_{22} - J_{33}}{J_{11}} x_5 \\ 0 & 0 & 0 & h \frac{J_{33} - J_{11}}{J_{22}} x_6 & 1 & 0 \\ 0 & 0 & 0 & 0 & h \frac{J_{11} - J_{22}}{J_{33}} x_4 & 1 \end{bmatrix},$$

$$B(x) = \begin{bmatrix} 0 & 0 & 0 \\ 0 & 0 & 0 \\ h/J_{11} & 0 & 0 \\ 0 & h/J_{22} & 0 \\ 0 & 0 & h/J_{33} \end{bmatrix}.$$

For Assumption 1, we know vector-valued continuous function library:

$$\begin{aligned} \xi_{A_1}(x) &= 1, \quad \xi_{A_2}(x) = 1, \quad \xi_{A_3}(x) = 1, \quad \xi_{A_4}(x) = (1, x_6), \\ \xi_{A_5}(x) &= \left(1, \sin x_1 \tan x_2, \cos x_1, \frac{\sin x_1}{\cos x_2}, x_4\right), \\ \xi_{A_6}(x) &= \left(1, \cos x_1 \tan x_2, \sin x_1, \frac{\cos x_1}{\cos x_2}, x_5\right), \\ \xi_{B_1}(x) &= 1, \quad \xi_{B_2}(x) = 1, \quad \xi_{B_3}(x) = 1. \end{aligned}$$

As in (39), the experimental inputs  $M_1 = \sin(50\pi t + \pi/10)$ ,  $M_2 = \sin(37\pi t + \pi/3)$ , and  $M_3 = \sin(21\pi t + \pi/2)$  are applied to collect data. A total of 20 experiments are performed, each lasting 1 second. The experimental noise  $d$  is randomly selected within the energy bound  $\Theta = 3.5 \times 10^{-5} I_6$  as in Assumption 2. Store the data samples into  $X_0$ ,  $X_1$ , and  $U_0$  as in (40). Take  $r = 0.4$  for  $\mathcal{B}_r$ . By (47), we have the set  $\bar{\mathcal{Q}}$  as in (48). Solving (53) in Theorem 4 via CVX yields

$$K = \begin{bmatrix} -2.8982 & -0.0671 & -0.0363 & -8.0286 & 0.0068 & 0.0012 \\ 0.0483 & -2.9979 & 0.0935 & 0.0041 & -8.7807 & -0.0053 \\ 0.0088 & -0.0988 & -4.8016 & 0.0001 & -0.0135 & -14.5194 \end{bmatrix}.$$

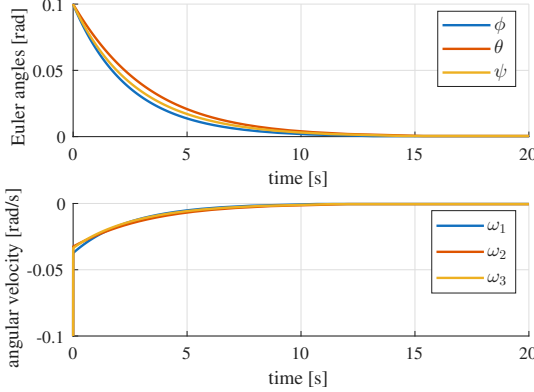


Fig. 8. State response of the closed-loop system in numerical simulation.

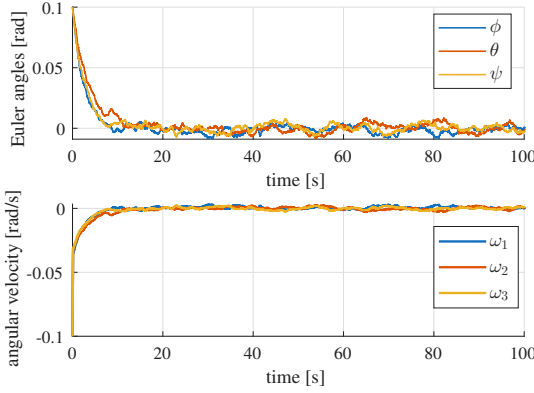


Fig. 9. State response of the closed-loop system under disturbance.

According to (57), the estimate of ROA,  $\mathcal{B}_{\bar{r}_0}$ , has a radius of  $\bar{r}_0 = 0.28061$ . As illustrated in Figure 8, the state response of the closed-loop system starting from initial value  $x(0) = (0.1, 0.1, 0.1, -0.1, -0.1, -0.1)$  converges to the origin.

For the closed-loop system  $x^+ = A(x)x + B(x)Kx + w$ , we set each component of  $w \in \mathbb{R}^6$  as a random variable uniformly distributed in the interval  $[-0.0002, 0.0002]$ . The simulation result is depicted in Figure 9, which is consistent with (59) in Theorem 5, demonstrating the robustness of the controller against disturbances.

### B. Physical Experiment

In this subsection, the data-driven controller is validated through a physical experiment under ROS and PX4 flight control framework [49]. The quadrotor aerial vehicle is mounted on a 3-degree-of-freedom rotational platform, as shown in Figure 10; thus, it follows the same attitude dynamics as in Section V-A. Under the PX4 framework, the control input  $u_i$  for  $i = 1, 2, 3$  is proportional to the torque, and the relationship is given by

$$\begin{bmatrix} M_1 \\ M_2 \\ M_3 \end{bmatrix} = \begin{bmatrix} c_1 & 0 & 0 \\ 0 & c_2 & 0 \\ 0 & 0 & c_3 \end{bmatrix} \begin{bmatrix} u_1 \\ u_2 \\ u_3 \end{bmatrix}.$$

The values of  $J$ ,  $c_1$ ,  $c_2$  and  $c_3$  are unknown to us.

We discretize the continuous-time system using the forward Euler method with a sampling time  $h = 0.002$ . The resulting discrete-time system, along with the known vector-valued

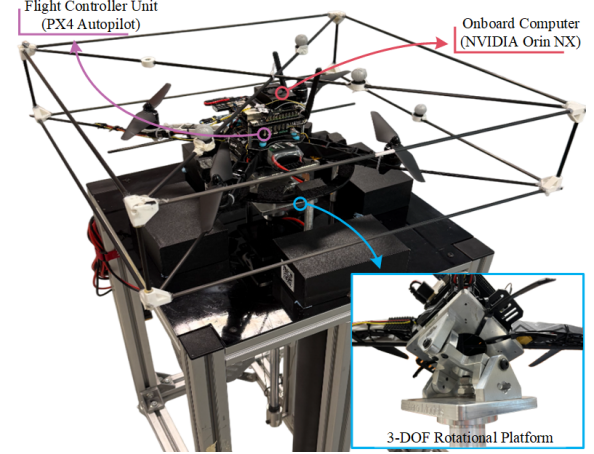


Fig. 10. Experimental setup. The quadrotor aerial vehicle is mounted on a 3-degree-of-freedom (3-DOF) rotational platform.

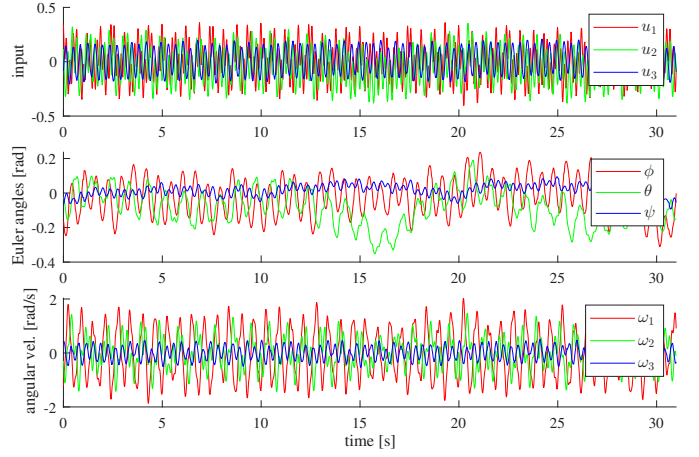


Fig. 11. Experimental data. First subfigure is the experimental input  $u_d$  as in (39), which is generated by a controller with degraded performance. The second and third subfigures show the corresponding state responses, namely the Euler angles and angular velocities, respectively.

continuous function library, is the same as in Section V-A, except for  $B(x)$ :

$$B(x) = \begin{bmatrix} 0 & 0 & 0 \\ 0 & 0 & 0 \\ 0 & 0 & 0 \\ hc_1/J_{11} & 0 & 0 \\ 0 & hc_2/J_{22} & 0 \\ 0 & 0 & hc_3/J_{33} \end{bmatrix}.$$

The collected experimental data is depicted in Figure 11, where the input  $u_d$  as in (39) is generated by a controller with degraded performance. Store the data samples into  $X_0$ ,  $X_1$  and  $U_0$  as in (40). The process noise  $D_0$  as in (40d) includes platform friction, sensor noise, motor nonlinearities, and aerodynamic disturbances, and is bounded by  $\Theta = 0.01I_6$  as in (42). Take  $r = 0.1$  for  $\mathcal{B}_r$ . By (47), we have the set  $\bar{\mathcal{Q}}$  as in (48). Solving (53) in Theorem 4 via CVX yields

$$K = \begin{bmatrix} -0.5722 & 0.0029 & -0.1327 & -0.1687 & -0.0068 & 0.1252 \\ -0.0531 & 0.8365 & 0.5700 & 0.0129 & 0.4564 & -0.1740 \\ 0.0210 & 0.1503 & 1.4681 & 0.0050 & -0.0164 & 1.3181 \end{bmatrix}.$$

According to (57), an estimate of ROA,  $\mathcal{B}_{\bar{r}_0}$ , has a radius of  $\bar{r}_0 = 0.0032264$ . The state response of the closed-loop system is illustrated in Figure 12. We note that various imperfections exist in the physical implementation, such as friction, noise,

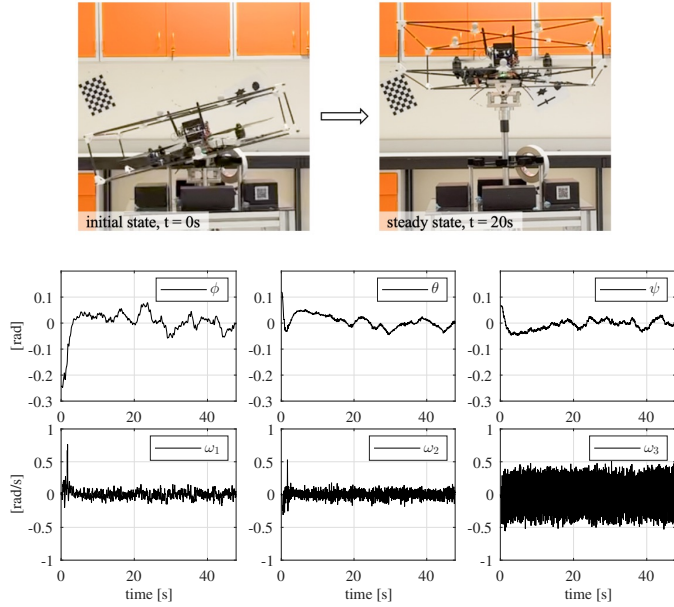


Fig. 12. State response of the closed-loop system.

motor nonlinearities, and aerodynamic disturbances. Consequently, the closed-loop states remain in the neighborhood of the origin, which aligns with (59) in Theorem 5, indicating the robustness of the data-driven controller against disturbances.

Additional demonstrations, which are not included here due to space limitations, are available at our project website [41] for interested readers.

## VI. CONCLUSION

In this paper, we have synthesized a controller for a nonlinear system directly from noisy data with rigorous end-to-end guarantees. Specifically, the state-dependent representation of a nonlinear system was utilized to derive model-based conditions for controller design. These conditions were subsequently adapted to the data-driven case. The resulting direct data-driven controller, with a guaranteed region of attraction, can stabilize all data-consistent nonlinear systems induced by data noise. Moreover, the closed-loop properties, namely robustness against disturbances and region of attraction under input saturation, were rigorously characterized based solely on data. This work focused on the state feedback stabilization problem. Future research includes nonlinear optimal control, output feedback control, and output regulation.

## REFERENCES

- A. Astolfi, “Nonlinear adaptive control,” in *Encyclopedia of Systems and Control*. Springer London, 2019, pp. 1–6.
- M. Campi and S. Savarese, “Direct nonlinear control design: the virtual reference feedback tuning (VRFT) approach,” *IEEE Transactions on Automatic Control*, vol. 51, no. 1, pp. 14–27, 2006.
- K. L. Moore, *Iterative Learning Control for Deterministic Systems*. Springer London, 2012.
- B. Kiumarsi, K. G. Vamvoudakis, H. Modares, and F. L. Lewis, “Optimal and autonomous control using reinforcement learning: A survey,” *IEEE Transactions on Neural Networks and Learning Systems*, vol. 29, no. 6, pp. 2042–2062, 2018.
- Z.-S. Hou and Z. Wang, “From model-based control to data-driven control: Survey, classification and perspective,” *Information Sciences*, vol. 235, pp. 3–35, 2013.
- G. Pillonetto, F. Dinuzzo, T. Chen, G. De Nicolao, and L. Ljung, “Kernel methods in system identification, machine learning and function estimation: A survey,” *Automatica*, vol. 50, no. 3, pp. 657–682, 2014.
- B. Recht, “A tour of reinforcement learning: The view from continuous control,” *Annual Review of Control, Robotics, and Autonomous Systems*, vol. 2, pp. 253–279, 2019.
- J. C. Willems, P. Rapisarda, I. Markovsky, and B. L. De Moor, “A note on persistency of excitation,” *Systems & Control Letters*, vol. 54, no. 4, pp. 325–329, 2005.
- C. De Persis and P. Tesi, “Formulas for data-driven control: Stabilization, optimality, and robustness,” *IEEE Transactions on Automatic Control*, vol. 65, no. 3, pp. 909–924, 2020.
- H. J. van Waarde, J. Eising, H. L. Trentelman, and M. K. Camlibel, “Data informativity: A new perspective on data-driven analysis and control,” *IEEE Transactions on Automatic Control*, vol. 65, no. 11, pp. 4753–4768, 2020.
- L. Li, A. Bisoffi, C. De Persis, and N. Monshizadeh, “Controller synthesis from noisy-input noisy-output data,” *Automatica*, vol. 183, p. 112545, 2026.
- J. Berberich, A. Koch, C. W. Scherer, and F. Allgöwer, “Robust data-driven state-feedback design,” in *2020 American Control Conference (ACC)*, 2020, pp. 1532–1538.
- I. Markovsky and F. Dörfler, “Behavioral systems theory in data-driven analysis, signal processing, and control,” *Annual Reviews in Control*, vol. 52, pp. 42–64, 2021.
- M. Guo, C. De Persis, and P. Tesi, “Data-driven stabilization of nonlinear polynomial systems with noisy data,” *IEEE Transactions on Automatic Control*, vol. 67, no. 8, pp. 4210–4217, 2022.
- A. Bisoffi, C. De Persis, and P. Tesi, “Data-driven control via Petersen’s lemma,” *Automatica*, vol. 145, p. 110537, 2022.
- H. Huang, M. K. Camlibel, R. Carloni, and H. J. van Waarde, “Data-driven stabilization of polynomial systems using density functions,” *arXiv preprint arXiv:2503.07092*, 2025.
- T. Dai and M. Sznaier, “A semi-algebraic optimization approach to data-driven control of continuous-time nonlinear systems,” *IEEE Control Systems Letters*, vol. 5, no. 2, pp. 487–492, 2021.
- M. Guo, C. De Persis, and P. Tesi, “Data-driven stabilizer design and closed-loop analysis of general nonlinear systems via taylor’s expansion,” *arXiv preprint arXiv:2209.01071*, 2023.
- T. Martin and F. Allgöwer, “Data-driven system analysis of nonlinear systems using polynomial approximation,” *IEEE Transactions on Automatic Control*, vol. 69, no. 7, pp. 4261–4274, 2024.
- P. Rapisarda, H. J. van Waarde, and M. Çamlibel, “Orthogonal polynomial bases for data-driven analysis and control of continuous-time systems,” *IEEE Transactions on Automatic Control*, vol. 69, no. 7, pp. 4307–4319, 2024.
- C. Fiedler, C. W. Scherer, and S. Trimpe, “Learning-enhanced robust controller synthesis with rigorous statistical and control-theoretic guarantees,” in *2021 60th IEEE Conference on Decision and Control (CDC)*, 2021, pp. 5122–5129.
- H. J. van Waarde and R. Sepulchre, “Kernel-based models for system analysis,” *IEEE Transactions on Automatic Control*, vol. 68, no. 9, pp. 5317–5332, 2023.
- Z. Hu, C. De Persis, and P. Tesi, “Learning controllers from data via kernel-based interpolation,” in *2023 62nd IEEE Conference on Decision and Control (CDC)*, 2023, pp. 8509–8514.
- T. Martin, T. B. Schön, and F. Allgöwer, “Guarantees for data-driven control of nonlinear systems using semidefinite programming: A survey,” *Annual Reviews in Control*, vol. 56, p. 100911, 2023.
- P. Bevanda, S. Sosnowski, and S. Hirche, “Koopman operator dynamical models: Learning, analysis and control,” *Annual Reviews in Control*, vol. 52, pp. 197–212, 2021.
- R. Strässer, M. Schaller, K. Worthmann, J. Berberich, and F. Allgöwer, “Koopman-based feedback design with stability guarantees,” *IEEE Transactions on Automatic Control*, vol. 70, no. 1, pp. 355–370, 2025.
- , “SafEDMD: A koopman-based data-driven controller design framework for nonlinear dynamical systems,” *arXiv preprint arXiv:2402.03145*, 2025.
- L. Fraile, M. Marchi, and P. Tabuada, “Data-driven stabilization of SISO feedback linearizable systems,” *arXiv preprint arXiv:2003.14240*, 2021.
- M. Alsatti, V. G. Lopez, J. Berberich, F. Allgöwer, and M. A. Müller, “Data-based control of feedback linearizable systems,” *IEEE Transactions on Automatic Control*, vol. 68, no. 11, pp. 7014–7021, 2023.

[30] C. De Persis, D. Gadginmath, F. Pasqualetti, and P. Tesi, “Feedback linearization through the lens of data,” *IEEE Transactions on Automatic Control*, pp. 1–13, 2025.

[31] C. De Persis, M. Rotulo, and P. Tesi, “Learning controllers from data via approximate nonlinearity cancellation,” *IEEE Transactions on Automatic Control*, vol. 68, no. 10, pp. 6082–6097, 2023.

[32] C. De Persis and P. Tesi, “Learning controllers for nonlinear systems from data,” *Annual Reviews in Control*, vol. 56, p. 100915, 2023.

[33] B. Samari and A. Lavaei, “Data-driven dynamic controller synthesis for discrete-time general nonlinear systems,” in *Proceedings of the 28th ACM International Conference on Hybrid Systems: Computation and Control*. Association for Computing Machinery, 2025.

[34] N. Monshizadeh, C. D. Persis, and P. Tesi, “A versatile framework for data-driven control of nonlinear systems,” *IEEE Transactions on Automatic Control*, pp. 1–8, 2025.

[35] T. Dai and M. Sznaier, “Nonlinear data-driven control via state-dependent representations,” in *2021 60th IEEE Conference on Decision and Control (CDC)*, 2021, pp. 5765–5770.

[36] X. Dai, C. De Persis, and N. Monshizadeh, “Online adaptation of data-driven controllers for unknown nonlinear systems,” *International Journal of Robust and Nonlinear Control*, 2025.

[37] C. M. Kellett and P. Braun, *Introduction to Nonlinear Control: Stability, Control Design, and Estimation*. Princeton University Press, 2023.

[38] Z.-P. Jiang and Y. Wang, “Input-to-state stability for discrete-time nonlinear systems,” *Automatica*, vol. 37, no. 6, pp. 857–869, 2001.

[39] S. Tarbouriech, G. Garcia, J. M. G. da Silva Jr., and I. Queinnec, *Stability and Stabilization of Linear Systems with Saturating Actuators*. Springer Science & Business Media, 2011.

[40] T. Çimen, “State-dependent riccati equation (SDRE) control: A survey,” *IFAC Proceedings Volumes*, vol. 41, no. 2, pp. 3761–3775, 2008, 17th IFAC World Congress.

[41] AxxBxu website. [Online]. Available: <https://nus-core.github.io/assets/standalone/AxxBxu/index.html>

[42] C. W. Scherer and S. Weiland, *Linear Matrix Inequalities in Control*. Lecture Notes, Dutch Institute for Systems and Control, Delft, The Netherlands, 2000.

[43] M. Grant and S. Boyd, *CVX: Matlab Software for Disciplined Convex Programming, version 2.1*. <http://cvxr.com/cvx>, Mar. 2014.

[44] A. Seuret and S. Tarbouriech, “Robust data-driven control design for linear systems subject to input saturation,” *IEEE Transactions on Automatic Control*, vol. 69, no. 9, pp. 6191–6198, 2024.

[45] D. Henrion and A. Garulli, *Positive Polynomials in Control*. Springer, 2005.

[46] R. Strässer, J. Berberich, M. Schaller, K. Worthmann, and F. Allgöwer, “Koopman-based control of nonlinear systems with closed-loop guarantees,” *at - Automatisierungstechnik*, vol. 73, no. 6, pp. 413–428, 2025.

[47] A. Isidori, *Nonlinear Control Systems*, 3rd ed. Springer London, 1995, published as eBook on April 17, 2013.

[48] B. Wie, *Space Vehicle Dynamics and Control*. American Institute of Aeronautics and Astronautics, 1998.

[49] K. Xiao, S. Tan, G. Wang, X. An, X. Wang, and X. Wang, “XTDrone: A customizable multi-rotor UAVs simulation platform,” *arXiv preprint arXiv:2003.09700*, 2020.